SOLID STATE DIVISION

TECHNICAL INFORMATION
SD-12

Characteristics and use of infrared detectors

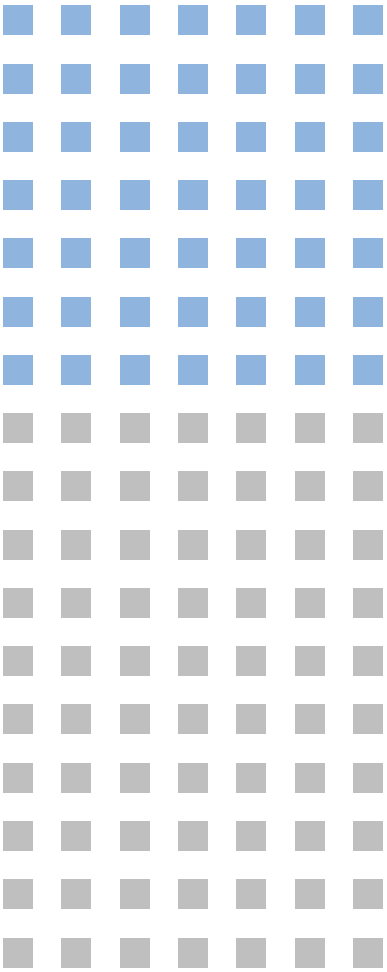

HAMAMATSU

Introduction

Infrared radiation consists of electromagnetic waves in the wavelength region from 0.75 µm to 1000 µm, lying between visible light and microwave light. In order to cover this broad spectrum of wavelengths, a variety of infrared detectors have been developed and produced.
This manual describes major characteristics and applications of Hamamatsu infrared detectors, including InGaAs PIN photodiodes, PbS and PbSe photoconductive detectors, InAs and InSb photovoltaic detectors, MCT (HgCdTe) photoconductive detectors, pyroelectric detectors, and hybrid detectors used in a combination of two or more detectors.
Custom-made detectors are also available upon request. Please feel free to consult Hamamatsu regarding your specific requirements.

Contents

1. Infrared radiation

Infrared radiation is the electromagnetic waves in the wavelength region longer than the visible light wavelengths, lying from 0.75 µm (1.65 eV) to 1000 µm (1.2 meV). The wavelength region of 0.75 µm to 3 µm is often called the near infrared, the wavelength region of 3 µm to 6 µm the middle infrared, and the wavelength region of 6 µm to 15 µm the far infrared. Also, even longer wavelength regions are sometimes referred to as ultra-far infrared, but this is not a universally accepted term.

Infrared radiation has the following characteristics:

(1) Invisible to human eyes
This is useful for security applications, but sometimes makes measurements and optical system design difficult.

(2) Small energy
Infrared radiation energy is equal to the vibrational or rotational energy of molecules. This phenomenon makes it possible to identify molecules.

(3) Long wavelength
This means infrared radiation is less scattered and offers better transmission through various medium.

(4) Emitted from all kinds of objects

1-1 Emission of infrared radiation

All objects with an absolute temperature of over 0 K emit infrared radiation. Infrared radiant energy is determined by the temperature and surface condition of an object. Suppose there is an object that absorbs all radiant energy and appears completely black at wavelengths. This object is called "blackbody". The following formula and laws can be established with regard to blackbodies.

1. **Blackbody spectral radiant emittance (Planck's radiation formula)**

$$M\lambda = C_1\lambda^{-5}[\exp(C_2/\lambda T) - 1]^{-1} \quad [W/cm^2\mu m]$$

T : Absolute temperature [K]
C_1: 1st radiation constant = 3.74×10^4 [$W\mu m^4/cm^2$]
C_2: 2nd radiation constant = 1.44×10^4 [µmK]
λ : Wavelength [µm]

2. **Stefan-Boltzmann law**

$$M = \sigma T^4 \quad [W/cm^2]$$

σ: Stefan Boltzmann's constant = 5.67×10^{-12} [W/cm^2K^4]

3. **Wien displacement law**

$$\lambda_{max}T = 2897.8 \quad [\mu mK]$$

λ_{max} : Maximum radiant wavelength [µm]

Figure 1-1 shows blackbody spectral radiant emittance. With regard to objects other than blackbodies, the following relation can be established.

$$M' = \varepsilon M$$

ε: emissivity

Emissivity ε varies with the surface condition of an object. It also usually varies with the wavelength and temperature of an object. Since emissivity is equivalent to absorbance, the emissivity of an object with large reflectance or transmittance becomes small. For more information, see section 12-3, "Radiation thermometer".

Figure 1-1 Blackbody spectral radiant emittance

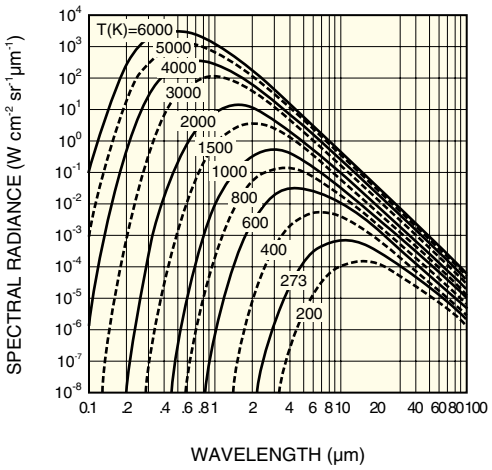

KIRDB0014EB

1-2 Infrared detection

Infrared radiation is used in a wide variety of applications, and new applications are constantly being developed. A typical system for detecting infrared radiation is usually configured as shown below.

1-2-1 Infrared sources

As stated above, all objects with an absolute temperature of over 0 K radiate infrared energy. For example, a human body at a temperature of 310 K (37 °C) radiates infrared energy with a peak wavelength of close to 10 µm. Infrared sources include blackbody radiators, tungsten lamps, silicon carbide, and other substances (see Table 1-1). In addition to these radiant sources, infrared lasers that emit infrared energy of a specific wavelength are used (see Figure 1-2).
In addition to the infrared source to be measured, there is background radiation from the ground at a temperature of 300 K. If the measurement system is required for a wavelength region over 3 µm, noise due to fluctuations in the background radiation will not be ignored. To reduce this type of noise, cold shields and cold filters are used in most cases.

Table 1-2 Types of infrared radiation sources [1)]

Type	Method	Material	Radiation source example	Wavelength (μm)	Remark
Thermal radiation	Resistor heating by current flow	Tungsten	Infrared bulb	1 to 2.5	Long wavelength region is cut off by external bulb (glass). Secondary radiation is emitted through the tube.
		Nichrome Kanthal	Electric heater	2 to 5	
		Silicon carbide (siliconate)	Globar	1 to 50	Constant voltage, large current
		Ceramic	Nernst glower	1 to 50	Pre-heating is needed.
	Secondary heating by other power source	Metal (stainless steel, etc.)	Sheath heater	4 to 10	
		Ceramic	IRS type lamp	4 to 25	
			Radiant burner	1 to 20	Heating by gas burning
	Heating by discharge	Carbon	Carbon arc lamp	2 to 25	Causes some environmental problems such as soot.
Cold radiation	Gas discharge	Mercury Cesium Xenon	Mercury lamp Xenon lamp	0.8 to 2.5	Long wavelength region is cut off by external bulb. Secondary radiation is emitted through the tube.
Stimulated emission	Laser reaction	Carbon dioxide Gallium arsenic compounds Lead compounds	CO_2 laser InGaAsP laser PbSnTe laser	9 to 11 1.1 to 1.5 6 to 7	

Figure 1-2 Wavelength regions of major infrared lasers

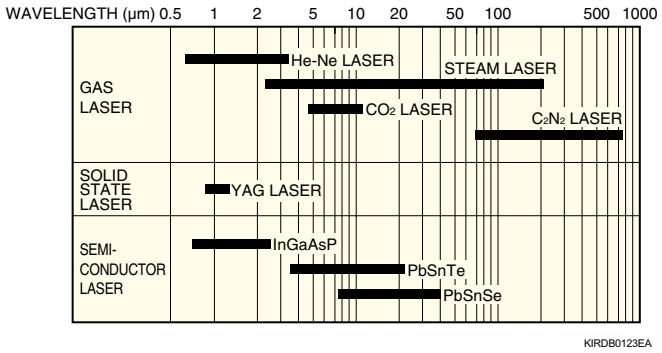

1-2-2 Transmission media

Typical examples of infrared transmission media include a vacuum, the atmosphere, and optical fibers. In the atmosphere, as shown in Figure 1-3, absorption by H_2O, CO_2, and other elements takes place at specific wavelengths. The bandwidths from 3 μm to 5 μm and from 8 μm to 12 μm, where the rate of absorption is lower, are sometimes called "atmospheric windows" and are often used for remote sensing applications. Optical fibers made of quartz with an attenuation factor that almost reaches the theoretical value has been developed, but other infrared fibers are still under improvement (see Figures 1-5).

Figure 1-3 Atmospheric absorption on sea surface [2)]

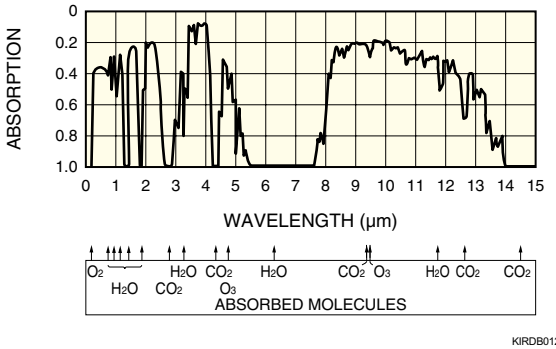

Figure 1-4 Atmospheric absorption at high altitude [3)]

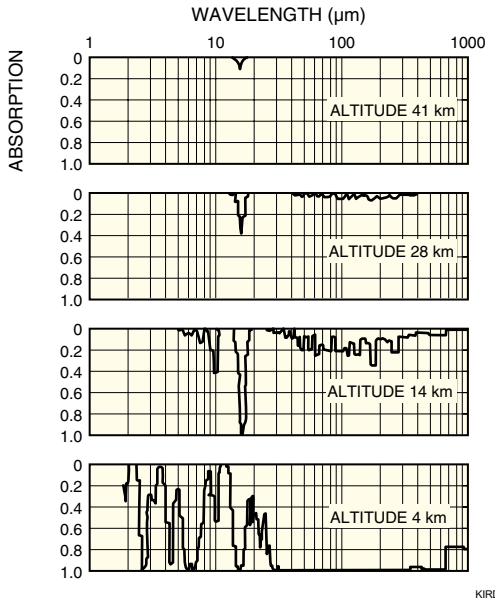

Figure 1-5 Theoretical transmission loss of optical fibers [4)]

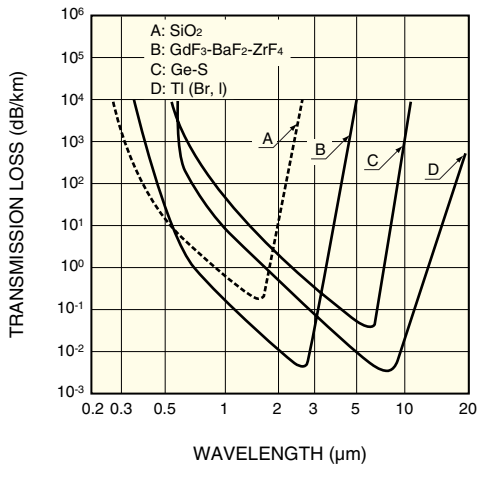

1-2-3 Optical materials

To converge or focus infrared radiation, optical lenses made of quartz, CaF_2, Ge and Si, polyethylene Fresnel lenses, and mirrors made of Al, Au or a similar material are used according to the wavelengths. Figure 1-6 shows the transmittance for typical infrared optical materials. In some applications, band-pass filters may be needed to utilize a specific wavelength, as well as choppers for passing and interrupting a beam of infrared radiation. When designing a band-pass filter, it is necessary to consider the center wavelength, half width (FWHM), and a 5% transmittance width. In addition, the side bands, meaning secondary transmission wavelengths other than the target wavelength, must also be considered, along with the transmittance at extraneous wavelengths, which is called "blocking". (See Figure 1-7.) Note that these characteristics vary with the temperature to be used and the angle of incident light.

Figure 1-6 Transmittance of various optical materials

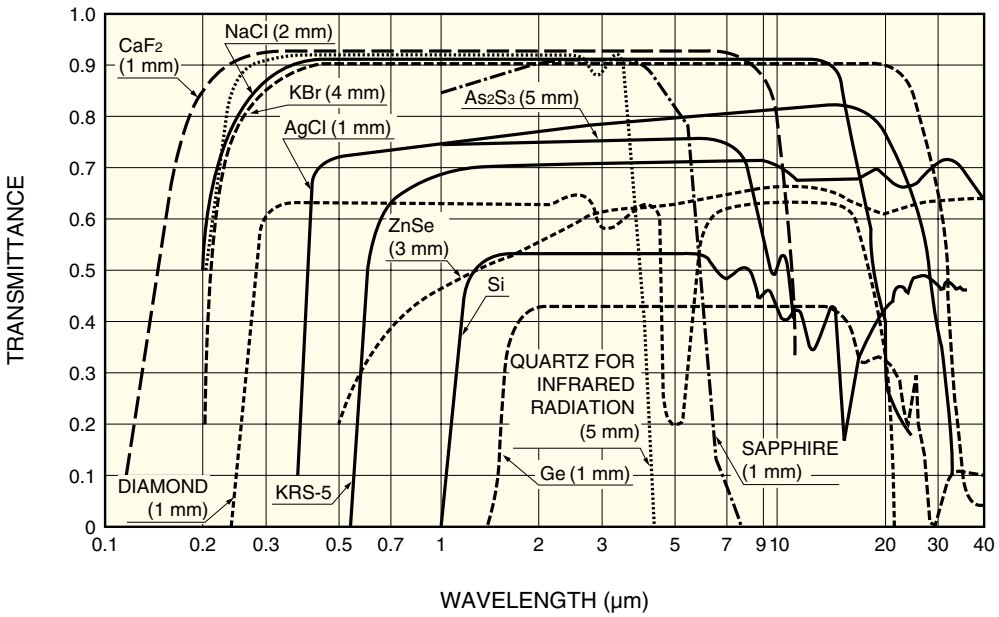

KIRDB0127EB

Figure 1-7 Example of band-pass filter transmittance

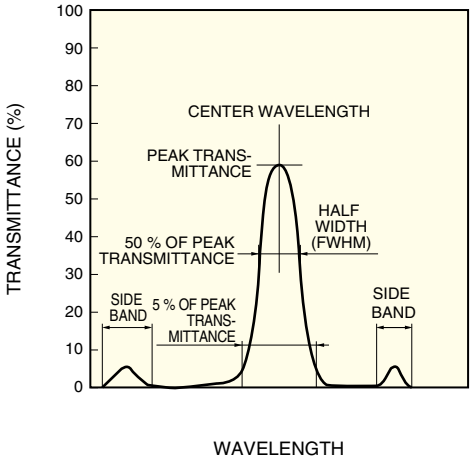

KIRDB0128EB

1-2-4 Detector elements

Hamamatsu manufactures two types of infrared detectors: a thermal type that has no wavelength dependence, and a quantum type that is wavelength-dependent. The energy of infrared radiation is expressed by the following equation:

$$E = \frac{hc}{\lambda} = \frac{1.24}{\lambda} \quad [eV]$$

h: Planck constant = 6.626×10^{-34} [J · s] = 4.14×10^{-15} [eV · s]
c: Speed of light = 3×10^{10} [cm/s]
l: Wavelength [µm]

In comparison with visible and ultraviolet rays, infrared radiation has small energy, for example 1.24 eV at 1 µm and 0.12 eV at 10 µm. To increase infrared detection efficiency, the detector should be cooled. Major characteristics indicating infrared detector performance are photo sensitivity, noise equivalent power (NEP) and D*.

(1) Photo sensitivity (Responsivity)

Photo sensitivity is the output voltage (or output current) per watt of incident energy when noise is not a consideration.

$$R = \frac{S}{PA} \quad [V/W]$$

S : Signal output [V]
P : Incident energy [W/cm^2]
A: Detector active area [cm^2]

Output signals from photovoltaic detectors are usually extracted as photocurrent, so the photo sensitivity is expressed in units of A/W. When light at a given wavelength enters a photovoltaic detector, the photocurrent Isc is expressed by the following equation.

$$Isc = \eta q \frac{PA}{h\frac{c}{\lambda}} = \frac{\eta q PA \lambda}{hc} \qquad (q: \text{electron charge})$$

Thus, photo sensitivity Rλ is as follows:

$$R\lambda = \frac{Isc}{PA} = \frac{\eta q \lambda}{hc} = \frac{\eta \lambda}{1.24} \qquad (\eta: \text{quantum efficiency})$$

and the relation with quantum efficiency η is as follows:

$$\eta = 1.24 \frac{R\lambda}{\lambda}$$

Output signals from photoconductive detectors are extracted as voltage by using a circuit like that shown below, the photo sensitivity is expressed in units of V/W.

Figure 1-8 Example of output signal measurement circuit for photoconductive detector

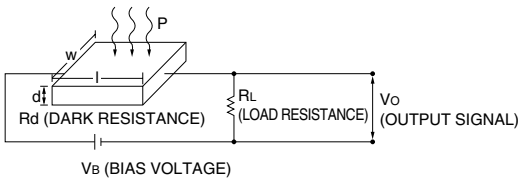

The output voltage Vo is defined by

$$Vo = \frac{RL}{Rd + RL} \cdot VB$$

A change in Vo due to changes in Rd when exposed to light becomes:

$$\Delta Vo = - \frac{RL\, VB}{(Rd + RL)^2} \cdot \Delta Rd$$

ΔRd is calculated as follows:

$$\Delta Rd = -Rd \frac{q(\mu e + \mu h)}{\sigma} \cdot \frac{\eta \tau \lambda PA}{lwdhc}$$

τ : Carrier lifetime
μe: Electron travel length
μh: Hole travel length
σ : Electrical conductance

thus the photo sensitivity is obtained as follows:

$$R\lambda = \frac{\Delta Vo}{PA} = \frac{q\eta\tau\lambda(\mu e + \mu h)}{\sigma lwdhc} \cdot \frac{RL\,Rd\,VB}{(Rd + RL)^2}$$

However, there are very few cases in which the quantum efficiency is determined using the above formulas, because Rd, μe, μh, τ and σ are quantities which are related to each other.

(2) Noise equivalent power: NEP

This is the quantity of incident light equal to the intrinsic noise level of a detector. In other words, this is the quantity of incident light when the signal-to-noise ratio (S/N) is 1.

$$NEP = \frac{PA}{S/N \cdot \sqrt{\Delta f}} \qquad [W/Hz^{1/2}]$$

N : Noise output [V]
Δf: Noise bandwidth [Hz]

(3) Detectivity: D* (D-star)

D* is the photo sensitivity per unit active area of a detector, which makes it easier to compare the characteristics of different detectors. In many detectors, NEP is proportional to the square root of the detector active area, so D* is defined by the following equation.

$$D^* = \frac{S/N \cdot \sqrt{\Delta f}}{P \cdot \sqrt{A}} = \frac{\sqrt{A}}{NEP} \qquad [cm \cdot Hz^{1/2}/W]$$

In general, the measurement conditions of D* are expressed in the format of D* (A, B, C), where A is the temperature [K] or wavelength [μm] of a radiant source, B is the chopping frequency, and C is the bandwidth. It can be said that a larger value of D* indicates a better detector element.

When selecting infrared detectors for your applications, it is necessary to consider wavelength, response time, cooling method, active area and shape, number of elements (single element, one-dimensional array, two-dimensional array, etc.) in addition to the above characteristics.

D* and peak sensitivity wavelength

When measuring infrared detector characteristics, a 500 K blackbody is often used as a radiant source. Between D* (500, f, 1) of this blackbody used as a radiant source and D* (λp, f, 1) at the peak sensitivity wavelength of a detector, the following relationship can be roughly established.

Figure 1-9 D* vs. peak sensitivity wavelength

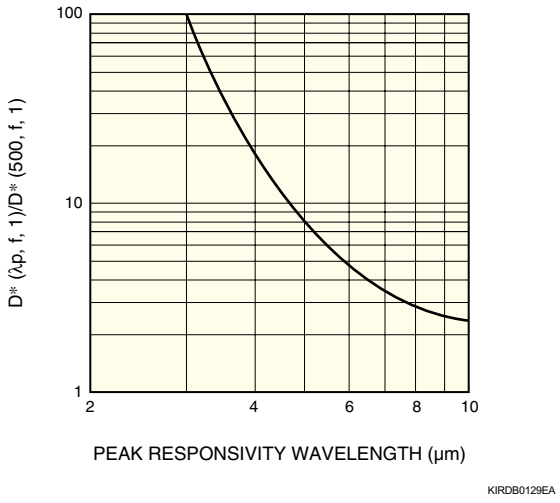

1-2-5 Signal processing

The signal output from a detector is generally quite small and needs to be amplified. When designing a preamplifier, it is necessary to consider an impedance that matches the detector, low noise, and bandwidth. If the incident light is modulated by a chopper, use of a tuned amplifier is effective in reducing the noise. If the detector is cooled, it is also practical to cool the amplifier. Figure 1-10 shows an example of a very low-light measurement circuit incorporating an InSb photovoltaic detector.

Figure 1-10 Example of signal processing circuit

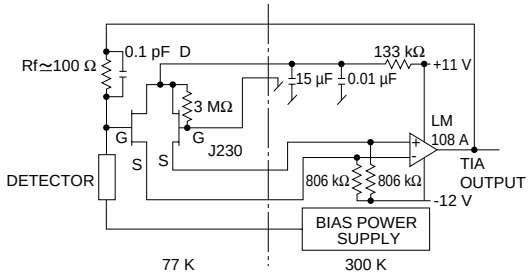

1-3 Applications using infrared radiation

Infrared radiation is used in a number of applications in the fields of industry, agriculture, medicine, science, communications, and remote sensing from space. Hamamatsu infrared detectors have been employed in a variety of fields as shown in Table 1-2. Some of these applications are described in Chapter 12, “Applications of infrared radiation” for your reference.

Table 1-2 Typical applications of Hamamatsu infrared detectors

Application \ Detector	InGaAs	PbS	PbSe	InAs	InSb	MCT	Two-color detector
Radiation thermometer	G8376-03	P9217 series	P791-11	P7163 P8079 series	P6606 series	P3981	K1713 series
HMD (Hot Metal Detectors)	G8376-03	P9217 series					
Flame monitors		P9217 series					K1713-01
Fire detectors			P791-11				K1713-02
Moisture analyzers	G8372-01 G8373-01	P2532-01 P2682-01 P9217 series					
Gas analyzer	G8371-01 G8372 -01 G8373 -01		P791-11 P2038-03 P2680-03	P8079 series	P5968 series P6606 series	P2750 P3981	
Spectrophotometer	G8371-01 G9211-256S G9212-512S G9213-256S G9214-512S G9208-256W	P2532-01 P2682-01		P7163 P8079 series	P4247-16 P5968 series	P3257 series P4249-08 P5274 P5274-01	K1713-05 K1713-09
Film thickness gauges			P791-11 P2038-03			P3257 series P3981	
Laser monitors	G8376 series G8941 series			P8079 series		P3257-30 P3257-31	K1713-05 K3413-05
Optical power meters	G8370-02 G8370-03 G8370-05						
Laser diode life test	G8370-01						
O/E converters	G8376-01 G8376-02 G6854-01						
FTIR				P8079 series	P5968 series	P3257 series P2748-40 P2748-41 P2748-42 P5274 P5274-01	
Thermal imaging					P4247-44 P5968 series	P2750 P3257 series P4249-08	
Remote sensing					P5968 series	P5138 series	
Human body detection							

2. Types of infrared detectors

Infrared detectors are classified into thermal types and quantum types. Thermal detectors use the infrared energy as heat and their photo sensitivity is independent of wavelength. Thermal detectors do not require cooling, but have disadvantages that response time is slow and detection capability is low.
In contrast, quantum detectors offer higher detection performance and a faster response speed, although their photo sensitivity is dependent on wavelength. In general, quantum detectors must be cooled for accurate measurement, except for detectors used in the near infrared region. Types of infrared detectors are shown in Table 2-1, and their typical spectral response characteristics are shown in Figure 2-1.

Table 2-1 Types of infrared detectors and their characteristics

Type			Detector	Spectral response (μm)	Operating temperature (K)	D^*(cm · Hz$^{1/2}$ / W)
Thermal type	Thermocouple · Thermopile			Depends on window material	300	D^* (λ,10,1) = 6×10^8
	Bolometer				300	D^* (λ,10,1) = 1×10^8
	Pneumatic cell		Golay cell, condenser-microphone		300	D^* (λ,10,1) = 1×10^9
	Pyroelectric detector		PZT, TGS, $LiTaO_3$		300	D^* (λ,10,1) = 2×10^8
Quantum type	Intrinsic type	Photoconductive type	PbS	1 to 3.6	300	D^* (500,600,1) = 1×10^9
			PbSe	1.5 to 5.8	300	D^* (500,600,1) = 1×10^8
			InSb	2 to 6	213	D^* (500,1200,1) = 2×10^9
			HgCdTe	2 to 16	77	D^* (500,1000,1) = 2×10^{10}
		Photovoltaic type	Ge	0.8 to 1.8	300	D^* (λp) = 1×10^{11}
			InGaAs	0.7 to 1.7	300	D^* (λp) = 5×10^{12}
			Ex. InGaAs	1.2 to 2.55	253	D^* (λp) = 2×10^{11}
			InAs	1 to 3.1	77	D^* (500,1200,1) = 1×10^{10}
			InSb	1 to 5.5	77	D^* (500,1200,1) = 2×10^{10}
			HgCdTe	2 to 16	77	D^* (500,1000,1) = 1×10^{10}
	Extrinsic type		Ge : Au	1 to 10	77	D^* (500,900,1) = 1×10^{11}
			Ge : Hg	2 to 14	4.2	D^* (500,900,1) = 8×10^9
			Ge : Cu	2 to 30	4.2	D^* (500,900,1) = 5×10^9
			Ge : Zn	2 to 40	4.2	D^* (500,900,1) = 5×10^9
			Si : Ga	1 to 17	4.2	D^* (500,900,1) = 5×10^9
			Si : As	1 to 23	4.2	D^* (500,900,1) = 5×10^9

Figure 2-1 Spectral response characteristics of various infrared detectors

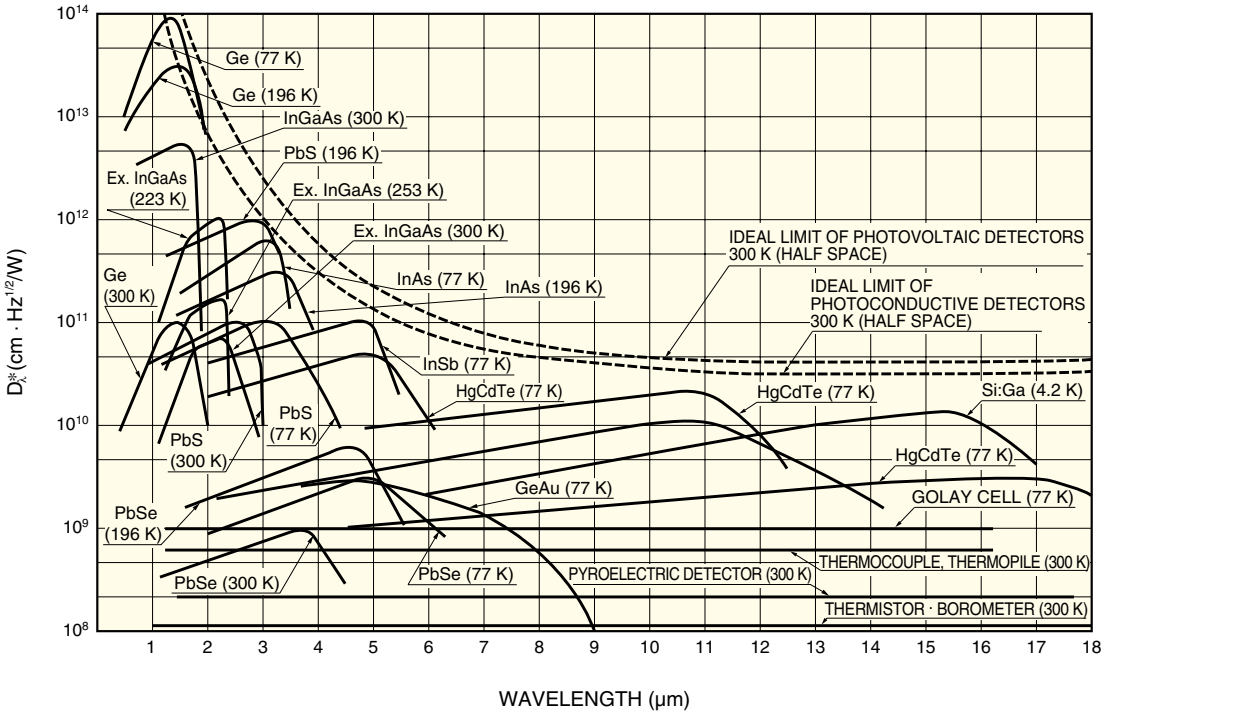

KIRDB0079EB

Theoretical limit of D*

Some noise occurs when detecting infrared radiation. This noise may come from the infrared detector itself, from its operating circuits or from background fluctuation. Suppose that noise from an infrared detector and its circuits can be ignored in comparison with the noise caused by background fluctuation. The detection limit is determined by only the noise from the background fluctuation. This is called "Background Limited Infrared Photodetection (BLIP)". The BLIPs of photovoltaic detectors and photoconductive detectors are given as follows:

$$\text{D* of photovoltaic detector} = D^*_\lambda = \frac{\lambda\sqrt{\eta}}{hc\sqrt{2Q}} \quad [\text{cm} \cdot \text{Hz}^{1/2}/\text{W}]$$

$$\text{D* of photoconductive detector} = D^*_\lambda = \frac{\lambda\sqrt{\eta}}{2hc\sqrt{Q}} \quad [\text{cm} \cdot \text{Hz}^{1/2}/\text{W}]$$

λ : Wavelength
η : Quantum efficiency
h : Planck constant
c : Speed of light
Q: Flux of background radiation

Figure 2-1 shows the BLIP of background radiation at 300 K when the FOV (field of view) = 180 °.

3. Selection guide

Hamamatsu manufactures and markets approximately 100 different types of infrared detectors. To select infrared detectors that suit your applications, please refer to the following selection guides.

(1) Wavelength region or temperature of the object to be measured

Referring to the spectral response characteristics in Figure 2-1 and the temperature limits in Table 3-1 will help you select the appropriate infrared detectors for your applications.

(2) Photo sensitivity and S/N (Signal-to-Noise)

Depending on the intensity of light signals and the type of information to be obtained, photo sensitivity and S/N required of infrared detectors differ, so the NEP and D* are used as guides to select the optimum infrared detectors. To improve the S/N, cooling the infrared detector will be necessary. There are several cooling methods: thermoelectric cooling, cryogenic cooling such as dry ice and liquid nitrogen, and mechanical cooling such as Stirling coolers. See “11. Cooling techniques” for how to cool the detectors. As you may notice from Figure 2-1, cooling changes the spectral response. The spectral response curves of PbS, PbSe and MCT photoconductive detectors shift to the longer wavelength side, while those of InGaAs PIN photodiodes, InAs and InSb photovoltaic detectors shift to the shorter wavelength side. The response time of PbS and PbSe photoconductive detectors becomes slower when cooled, so take precautions when cooling these detectors. As stated previously, the spectral response can chiefly be evaluated in terms of the following three characteristics.

● Photo sensitivity

This represents the magnitude of photo sensitivity (voltage or current) per watt of incident light. The photo sensitivity of photoconductive type detectors is expressed in V/W, and the photo sensitivity of photovoltaic type detectors is expressed in A/W.

● NEP (Noise Equivalent Power)

This represents the detection ability of a detector and is expressed in the quantity of incident light equal to the quantity of noise, i.e., the quantity of the incident light in which its S/N becomes unity.

● D* (Detectability)

D* is a measure of the S/N of a detector when infrared radiation of 1 W is input through an optical chopper. Since D* is independent of the active area and shape of the detector element, it is convenient when comparing characteristics of the detector element materials.

D* is usually measured by normalizing the detector active areas to 1 cm^2 and setting the amplifier bandwidth to 1 Hz. Measurement conditions of D* are expressed in the form of D* (A, B, C), where A is the temperature of a light source (K) or wavelength (μm), B is the chopping frequency (Hz), and C is the noise bandwidth (Hz). The units are $cmHz^{1/2}/W$. The higher the value of D*, the better the detection capability.

(3) Response speed and chopping frequency

Response speeds required of infrared detectors depend on their applications. For example, optical communications require a response speed of 1 GHz, and intrusion detection alarms require a response speed of 0.1 Hz. It is essential to select an appropriate infrared detector with the response speed and chopping frequency that suits your applications.

(4) Active area size and the number of elements

Depending on the optical systems in your application, you may need to determine the size and geometry of an active area and also use a single detector, linear array or 2-D array. InGaAs PIN photodiodes, PbS and PbSe photoconductive detectors, InSb photovoltaic detectors and MCT photoconductive detectors are relatively flexible in terms of geometry, size and the number of elements.

(5) Package

Packages used for infrared detectors are divided into metal can package, ceramic package, DIP types and Dewar types (glass or metal).

Also, depending on the application, the linearity, stability, temperature characteristics, price and other elements become important factors for selection.

Figure 3-1 Package examples

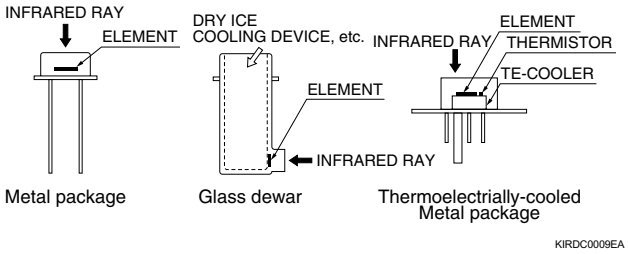

Table 3-1 Measurement temperature limit guides of infrared detectors

Measurement temperature limit	Infrared detector
600 ˚C	Si
200 ˚C	InGaAs
100 ˚C	PbS
50 ˚C	PbSe
0 ˚C	InSb
-50 ˚C	MCT, pyroelectric detector

4. InGaAs PIN photodiode

InGaAs PIN photodiodes are photovoltaic detectors having p-n junctions just like Si photodiodes. Since InGaAs PIN photodiodes have a smaller energy gap than Si photodiodes, they have sensitivity in the longer wavelength range than Si photodiodes. The energy gap of InGaAs PIN photodiodes varies as shown in Figure 4-1 depending on the composition ratio of In and Ga. By changing the composition ratio, it is possible to manufacture infrared detectors with various spectral response ranges In addition to the standard type having a long wavelength cut-off at 1.7 µm, Hamamatsu also provides longer wavelength types having cutoffs at 1.9 µm, 2.1 µm and 2.6 µm.

Figure 4-1 Relation between In_{1-x} Ga_x As lattice constant and energy gap

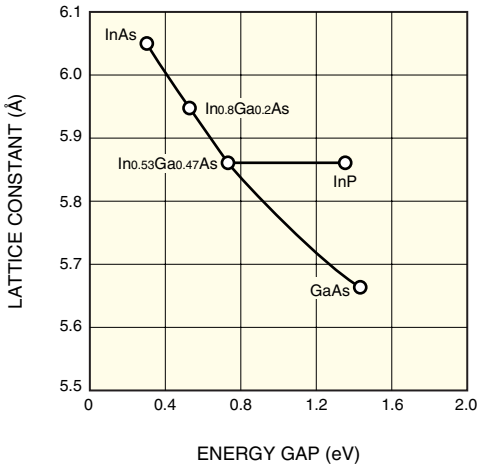

4-1 Characteristics

4-1-1 Voltage-current characteristic

When a voltage is applied to an InGaAs PIN photodiode in darkness, a voltage-current characteristic like that shown in Figure 4-2 (a) is obtained. When incident light enters the InGaAs PIN photodiode, the voltage-current characteristic curve becomes as shown in 2 of Figure 4-2 (b). When much stronger incident light enters, the curve shifts as shown in 3 of Figure 4-2 (b). Here, when both terminals of the photodiode are left open, a forward voltage Vop appears, and when both terminals are shorted, a current of Isc flows in the reverse direction.

Figures 4-3 (a) and (b) show how light can be measured by measuring the photoelectric current. The method shown in Figure 4-3 (a) uses an amplifier with a gain of G to amplify the voltage of ($I_o \times R_L$). In this case, the circuit linearity range is limited (see Figure 4-2 (c)).

The other method shown in Figure 4-3 (b) uses an operational amplifier. Supposing the open loop gain of the operational amplifier is "A", the equivalent input resistance expressed as Rf/A due to the negative feedback circuit becomes several digits smaller. Thus, an ideal Isc measurement is possible with this method. When measuring Isc over a wider range, change the Rf value as necessary.

Figure 4-2 Voltage-current characteristics

(a) In darkness

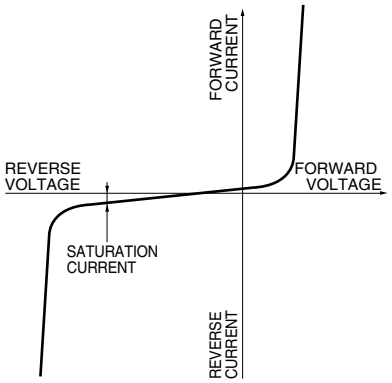

(b) Illuminated

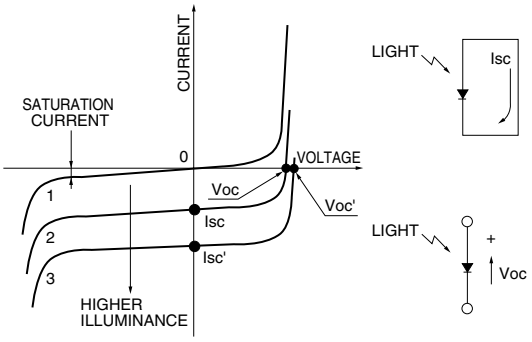

(c) Current-voltage characteristic and load line

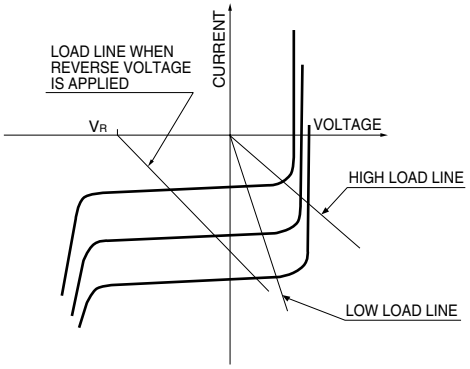

Figure 4-3 Photodiode operation circuits

(a) When used with reverse voltage

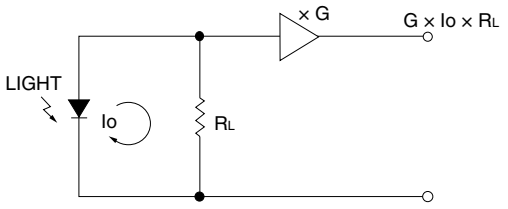

(b) When used with operational amplifier

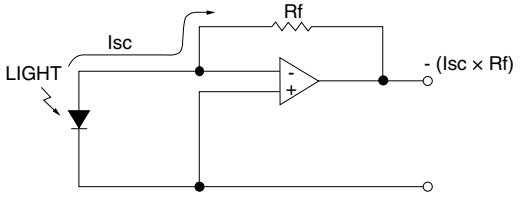

KPDC0006EA

4-1-2 Equivalent circuit

The equivalent circuit of an InGaAs PIN photodiode is shown in Figure 4-4. From this equivalent circuit, the short circuit current (Isc) is given by the following formula. The limit of Isc linearity is determined by the 2nd and 3rd terms of this formula.

$$Isc = I_L - Is\left[\exp\frac{q(Isc \cdot Rs)}{kT} - 1\right] - \frac{Isc \cdot Rs}{Rsh} \quad \cdots\cdots\cdots\cdots (4\text{-}1)$$

q : Electron charge
k : Boltzmann constant
T : Absolute temperature of element
Is : Saturation current of photodiode in the reverse direction

Figure 4-4 Equivalent circuit of InGaAs PIN photodiode

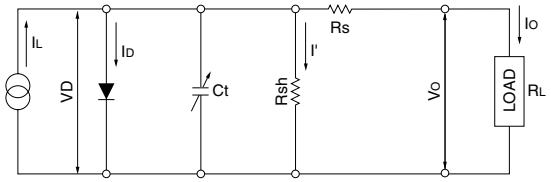

KPDC0004EA

I_L : Current generated by incident light (Proportional to the quantity of light)
I_D : Diode current
Ct : Terminal capacitance
Rsh : Shunt resistance
Rs : Series resistance
I' : Shunt resistance current
V_D : Voltages across the diode
Io : Output current
Vo : Output voltage

4-1-3 Linearity

As shown in Figure 4-5 (a), the lower limit of the linearity of InGaAs PIN photodiodes is determined by noise, while the upper limit is determined by the detector active area and the electrode structure. To expand the upper limit, it is sometimes practical to apply a bias voltage. Where only the linearity is a consideration, applying 1 V is sufficient. Figure 4-6 shows practical examples for bias voltage application. In this mode, the InGaAs PIN photodiode is used as a photoconductive detector. Applying a bias voltage is effective in improving the linearity and response speed, but this also increases the dark current and noise level. Moreover, an excessive bias voltage may damage InGaAs PIN photodiodes and deteriorate their performance. Always use them within the maximum rating voltage and set so that the cathode has a positive potential with respect to the anode.

Figure 4-5

(a) Linearity

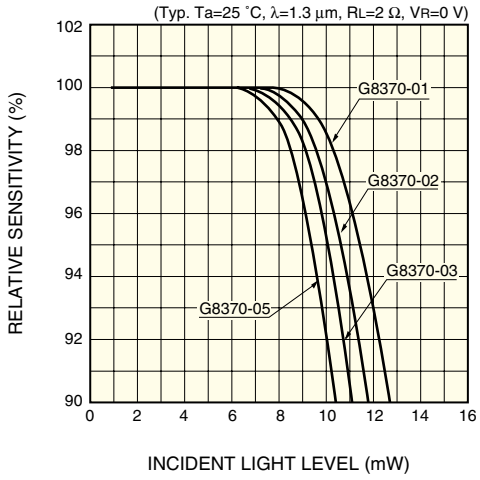

KIRDB0245EA

(b) Linearity with bias voltage applied

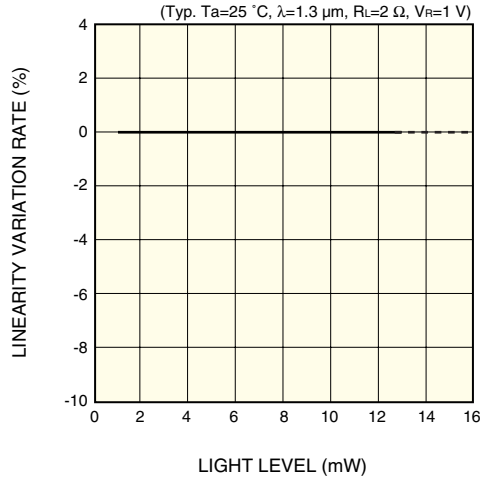

KIRDB0131EA

Figure 4-6 Example of bias voltage application

(a)

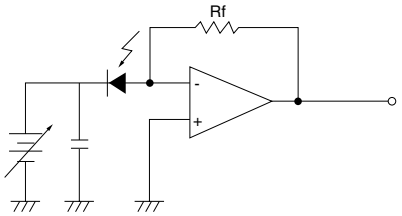

(b)

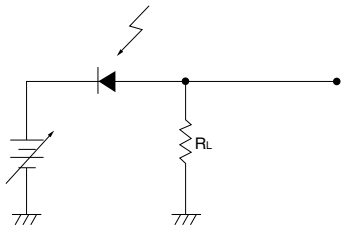

KIRDC0031EA

4-1-4 Noise characteristics

Like other types of photodetectors, the detection limit of InGaAs PIN photodiodes is determined by the noise characteristics. The noise current "in" of an InGaAs PIN photodiode can be expressed by the sum of the thermal noise (or Johnson noise) "ij" of the resistance which can be approximated by the shunt resistance "Rsh" and the shot noises "i_{SD}" and "i_{SL}" caused by the dark current and the photocurrent.

$$in = \sqrt{ij^2 + i_{SD}^2 + i_{SL}^2} \quad [A] \quad \cdots\cdots (4\text{-}2)$$

In the case where the reverse voltage is not applied as shown in Figure 4-3, ij is given by the following formula.

$$ij = \sqrt{\frac{4kTB}{Rsh}} \quad [A] \quad \cdots\cdots (4\text{-}3)$$

k : Boltzmann constant
T: Absolute temperature of the element
B: Noise bandwidth

In the case where the reverse voltage is applied as shown in Figure 4-6, the dark current always exists and i_{SD} is given by the following formula.

$$i_{SD} = \sqrt{2qI_DB} \quad [A] \quad \cdots\cdots (4\text{-}4)$$

q : Electron charge
I_D: Dark current
B : Noise bandwidth

On the other hand, when the optical current "I_L" flows by input of light, and $I_L >> 0.026/Rsh$ or $I_L >> I_D$, formula (4-5) of the shot noise "i_{SL}" is used instead of (4-3) or (4-4).

$$isl = \sqrt{2qI_LB} \quad \cdots\cdots (4\text{-}5)$$

As the level of the noise current is proportional to the square root of the measurement bandwidth "B", it is expressed in the unit of A/HZ$^{1/2}$ normalized by "B". In general, the detection limit of a photodetector is expressed by using the incident light that produces a signal current equal to a noise current expressed by formula (4-3) or (4-4), which is called the "Noise Equivalent Power (NEP)."

$$NEP = \frac{in}{S} \quad [W / Hz^{\frac{1}{2}}] \quad \cdots\cdots (4\text{-}6)$$

in: Noise current
S : Photo sensitivity

When using a circuit configuration as shown in Figure 4-3 (b), it is necessary to consider the noise of the operational amplifier and Rf in addition to the noise from the InGaAs PIN photodiode described previously. Furthermore, some applications in the high-frequency region require transmission factors such as the photodiode capacitance Ct and feedback capacitance Cf to be considered. The detection limit becomes larger than the value of NEP which is expressed by formula (4-6) above, as it is affected by the temperature drift of the amplifier, flicker noises in the low-frequency region and gain peaking which will be described in a later section.
An effective method to improve the detection limit is use of a cooled type InGaAs PIN photodiode. Also, if only those signals of the applicable frequency are detected synchronously by turning the incident light on and off periodically by some means, noise in the unwanted region can be avoided, making it possible to approximate the detection limit closer to the NEP value. (Figure 4-7)

Figure 4-7 Synchronous measurement technique

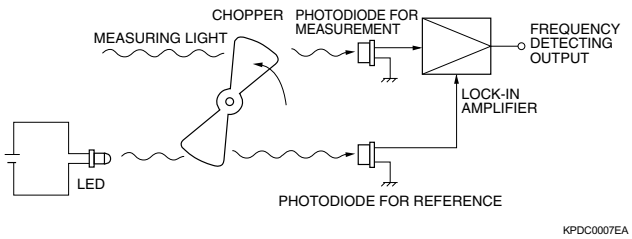

KPDC0007EA

4-1-5 Spectral response

There are two types of InGaAs PIN photodiodes. One is a standard type whose cut-off wavelength is 1.7 µm and the other is a long wavelength type with longer cut-off wavelengths. Their spectral response characteristics are shown in Figures 4-8 (a) and (b). The detection limit wavelength can be calculated by using the band gap energy Eg in the following formula.

$$\lambda c\ [\mu m] = \frac{1.24}{Eg} \quad [eV] \quad \cdots\cdots (4\text{-}7)$$

The band gap energy Eg of a standard InGaAs light absorbing layer is 0.73 eV. With the long wavelength type, the Eg is made smaller by changing the composition ratio of the InGaAs PIN

light absorbing layer and thus the detection limit wavelength is extended to the long wavelength region.
As the temperature decreases, the spectral response range of InGaAs PIN photodiodes shifts to the short wavelength region. However, the noise level also lowers with the decreasing temperature, so D* becomes large as shown in Figures 4-9 (a) and (b).

Figure 4-8 Spectral response

(a) Standard type

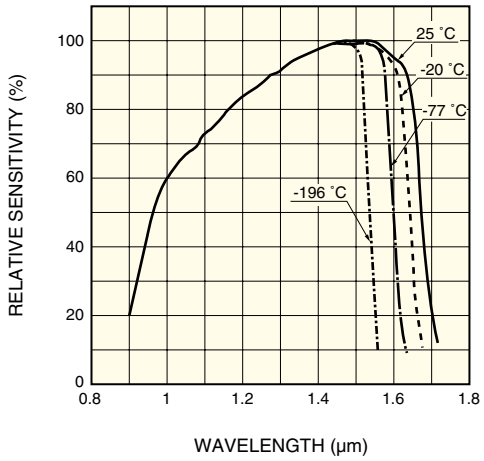

KIRDB0132EA

(b) Long wavelength type

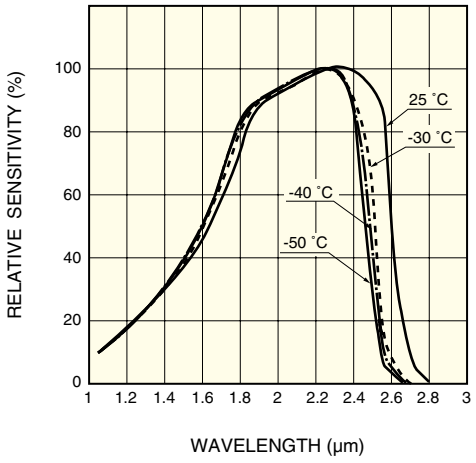

KIRDB0133EA

Figure 4-9 D* vs. wavelength

(a) Standard type

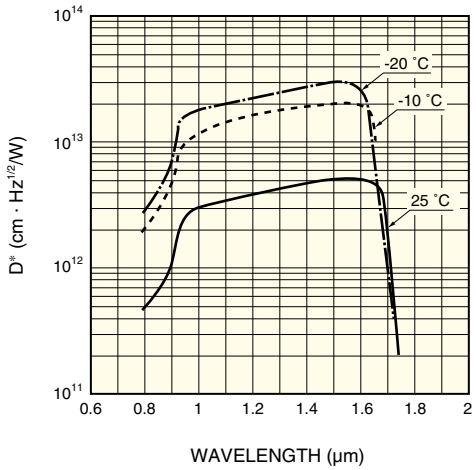

KIRDB0134EA

(b) Long wavelength type

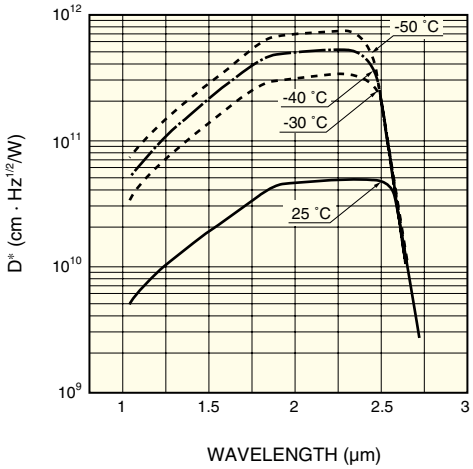

KIRDB0135EA

4-1-6 Time response characteristic

Response speed is the value that exhibits how fast the generated carrier flows to external circuits as a current. The response speed is expressed in rise time "tr" at which an output signal rises from 10 % to 90 % of its peak value. The following relation lies among tr, Ct, R_L and Rs.

$$tr = 2.2Ct\,(R_L + Rs) \quad \cdots\cdots (4\text{-}8)$$

Generally Rs can be disregarded because R_L>Rs. To make the rise time tr small, Ct and R_L should be made small. But R_L is determined by an external factor, and so cannot freely be moved at will. It is therefore necessary to make Ct small. Ct is proportional to the active area A but inversely proportional to the square root of bias voltage (reverse voltage V_R), which is given by the following formula.

$$Ct \propto \frac{A}{\sqrt{V_R}} \quad \cdots\cdots (4\text{-}9)$$

Faster response speeds can therefore be obtained by applying a reverse bias to a photodiode having a small active area. Also, the electric charge generated by light absorbed outside the p-n junction sometimes takes over several microseconds to diffuse and reach the electrode. When the time constant of Ct × RL is small, this diffusion time determines the response time.
When a high-speed response is needed, care should be taken so that the light does not fall outside the active area.
The relation between the rise time tr and cut-off frequency fc (Hz) is t =0.35 / fc.

Figure 4-10 Terminal capacitance vs. reverse voltage

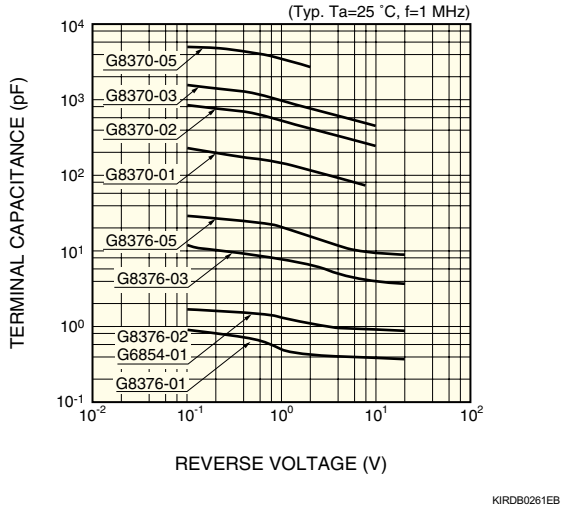

Figure 4-11 shows a high-speed detection circuit using an InGaAs PIN photodiode, which is a specific example of Figure 4-6 (b) with a 50 Ω load resistance included. The ceramic capacitor C is used to reduce the internal resistance of the reverse voltage power source and the resistor R to protect the photodiode. The voltage drop caused by the maximum photocurrent is selected in the much smaller range than the reverse voltage. Connections of leads for the photodiode and capacitor, the core wire of the coaxial cable and other wires where high-speed pulses pass through should be kept as short as possible.

Figure 4-11 High-speed photodetection circuit

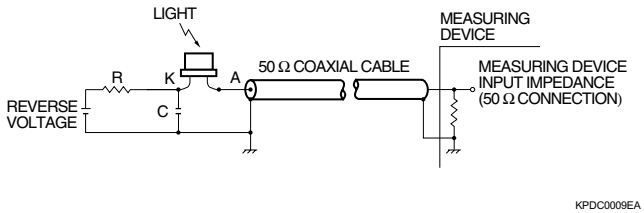

4-1-7 Temperature characteristics

As stated in 4-1-5, "Spectral response", spectral response characteristics vary with detector temperature. Temperature characteristics of shunt resistance Rsh are shown in Figure 4-12. Since the shunt resistance Rsh increases as the detector temperature decreases, the S/N can be improved by cooling the detector. Thermoelectrically-cooled type InGaAs PIN photodiodes are available for operation at a constant temperature (or cooled temperature). These types have one-stage or two-stage thermoelectric cooling element and a thermistor sealed in the same package. See Section 11 for more information on cooling techniques.

Figure 4-12 Shunt resistance vs. temperature

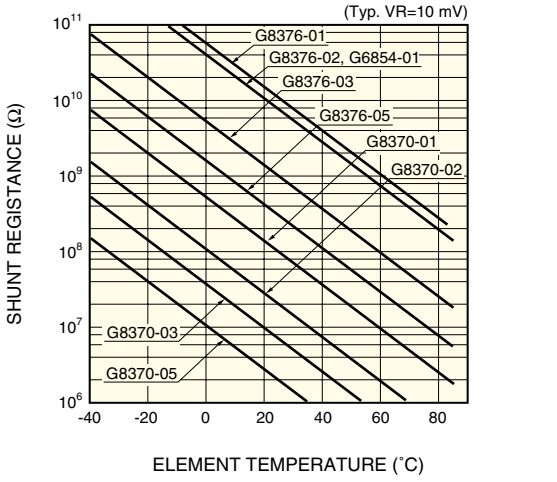

4-2 How to use

4-2-1 Connecting to the operational amplifier

The input impedance of the operational amplifier circuit shown in Figure 4-13 is the value equal to feedback resistance Rf divided by open gain and therefore becomes a very small value to approximate the operation of short-circuit current Ish, thus resulting in excellent linearity. Some precautions for use of the operational amplifiers are noted below.

Figure 4-13 Basic connection diagram

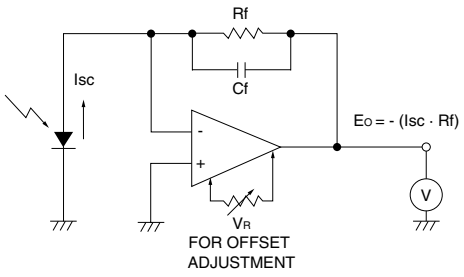

● **Feedback resistance**

In Figure 4-13, the output of photocurrent becomes the voltage of Isc × Rf (current-voltage conversion).

The feedback resistance Rf is determined by Isc and the required output voltage Vo. When it becomes larger than the shunt resistance, the input noise voltage and input offset voltage of the operational amplifier are multiplied by (1+ Rf/Rsh) and the result is superimposed over the output voltage. As the bias current error of the operational amplifier also becomes large, the feedback resistance should not be allowed to increase without limit. The feedback capacitance Cf is sometimes called the "damping capacitance" and is used mainly for oscillation protection. In some cases, a few pF is sufficient for this protection. This feedback circuit has a time constant of Cf × Rf and serves as a noise filter. However, at the same time it constrains the response speed, and so it is necessary to select values that suit your applications. Also, the error caused by offset voltage can be reduced to below 1 mV by connecting a variable resistor to the offset adjustment terminal of the operational amplifier.

● **Selecting the operational amplifier**

The actual input resistance of the operational amplifier is not infinite and some bias current flows into and out of the input terminal, potentially causing an error, depending on the level of the detection current. Such bias current ranges from several nA to several hundred nA in the case of a bipolar operational amplifier and is below several 0.1 pA in the case of an FET input type operational amplifier.

Generally, the bias current of the FET type operational amplifier is doubled when the temperature rises by 10 °C, but it decreases with a bipolar operational amplifier. For this reason, when designing a high-temperature circuit, use of a bipolar type operational amplifier should be considered. Also, like offset voltage, the error voltage caused by the bias current can be fine-adjusted by connecting a variable resistor to the offset adjustment terminal of the operational amplifier.

5. InGaAs linear image sensor

The InGaAs linear image sensor is a self-scanning photodiode array designed specifically for detectors in multichannel spectroscopy. The InGaAs PIN linear image sensor offers a number of features necessary for detectors in multichannel spectroscopy, for example a large photosensitive area, high quantum efficiency, wide dynamic range due to low dark current and high saturation charge, excellent output linearity and uniformity, as well as low power consumption. The standard types use a sapphire window that has superior infrared transmission. Applications include not only spectroscopy but also a wide range of image readout systems.

Hamamatsu InGaAs liner image sensors have the following features.

- **Uses the charge integration method in which the InGaAs active area is handled simply as a current source. This allows the InGaAs photodiodes in the active area to operate at low bias, resulting in outstanding performance as an image sensor.**
- **Two wavelength ranges of 0.9 to 1.7 µm and 0.9 to 2.6 µm are provided.**
- **InGaAs active area fabricated in a highly stable production process allows an extremely small dark current level and a long exposure time, making it ideal for low-light-level detection.**
- **Built-in thermoelectric coolers make temperature control and cooling easy.**

Figure 5-1 InGaAs linear image sensor active area and cross section

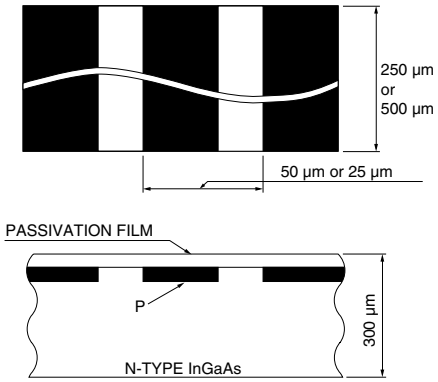

KIRDC0032EA

Figure 5-2 Spectral response

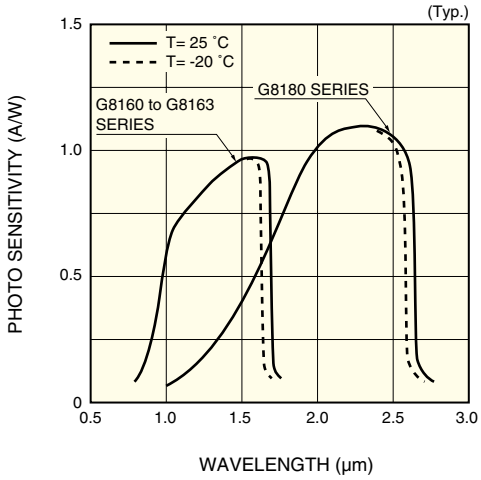

KIRDB0120EA

Table 5-1 Typical InGaAs linear image sensors

Parameter	G8160-256S	G8161-512S	G8162-256S	G8163-512S	G8180-256W	Unit
Spectral response range	0.9 to 1.7				0.9 to 2.6	µm
Cooling type	Non-cooled				Two-stage TE-cooled	-
Number of pixels	256	512	256	512	256	-
Pixel pitch	50	25	50	25	50	µm
Pixel height	250		500		250	µm
Package	28-pin DIP					-
Package length	63.5					mm
Window material	Sapphire					-

6. PbS, PbSe photoconductive detector

PbS and PbSe photoconductive detectors are infrared detectors making use of the photoconductive effect that resistance is reduced when infrared radiation enters the detecting elements. Compared with other detectors in the same wavelength region, the PbS and PbSe have superior features, such as higher detection capability, faster response speed, and they also operate at room temperatures. However, the dark resistance, photo sensitivity and response characteristics change depending on the ambient temperature. Therefore, care is required to ensure the best results.

6-1 Characteristics

6-1-1 Spectral response

Unlike other semiconductors, the temperature characteristics of PbS and PbSe band gaps have a negative coefficient. Because of this, the spectral response characteristics shift to the long wavelength region when cooled.

Figure 6-1 Spectral response (PbS)

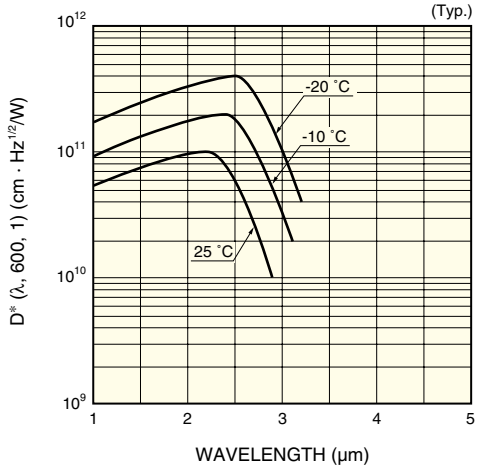

KIRDB0265EA

Figure 6-2 Spectral response (PbSe)

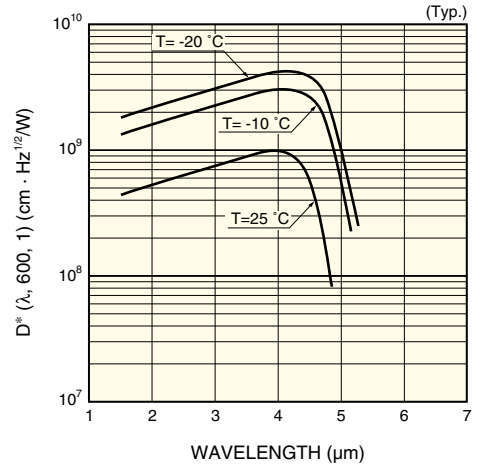

KIRDB0051EA

6-1-2 Time response characteristics

The frequency responses of the PbS and PbSe can be obtained from the following formula.

$$R(f) = \frac{R(o)}{\sqrt{1 + 4\pi^2 f^2 \tau^2}} \qquad [V]$$

R(f) : Frequency response
R(o): Response at zero frequency
f : Chopping frequency
τ : Time constant

Since the PbS and PbSe have typical 1/f noise spectra, D* becomes:

$$D^*(f) = \frac{k\sqrt{f}}{\sqrt{1 + 4\pi^2 f^2 \tau^2}}$$

Thus, D* (f) is maximized when $f = \frac{1}{2\pi\tau}$.

The frequency characteristics of PbS and PbSe photoconductive detectors are as shown in Figures 6-3 and 6-4. Also, Figure 6-7 shows the frequency characteristic of the PbS at room temperatures (+25 °C), at thermoelectrically-cooled temperature (-20 °C).

Figure 6-3 S/N vs. chopping frequency (PbS)

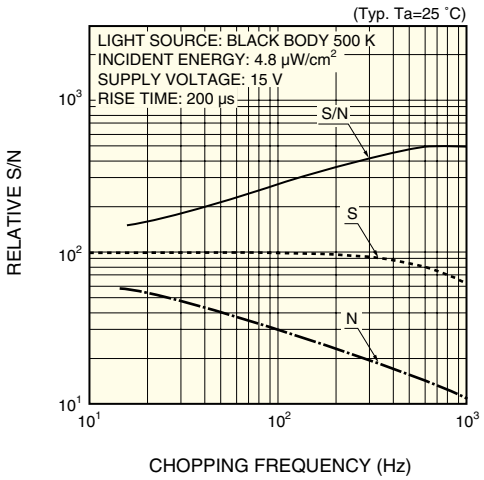

KIRDB0047EA

Figure 6-4 S/N vs. chopping frequency (PbSe)

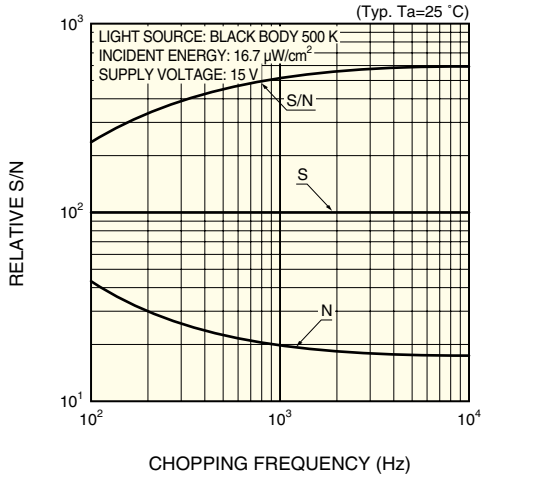

Figure 6-5 Linearity (PbS)

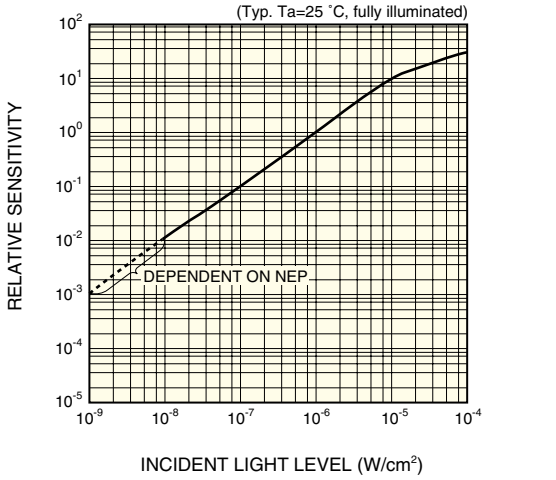

Figure 6-6 Linearity (PbSe)

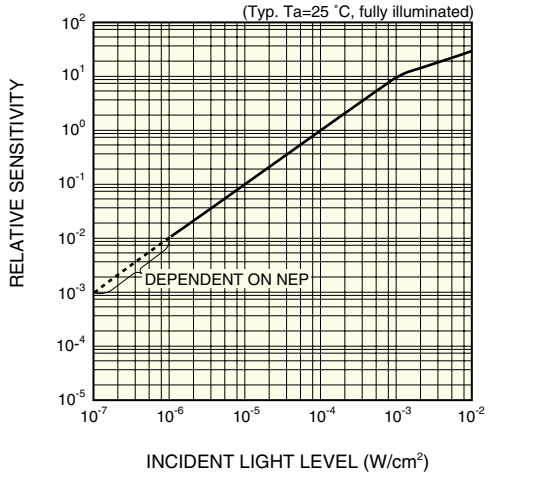

Figure 6-7 Photo sensitivity vs. chopping frequency (PbS)

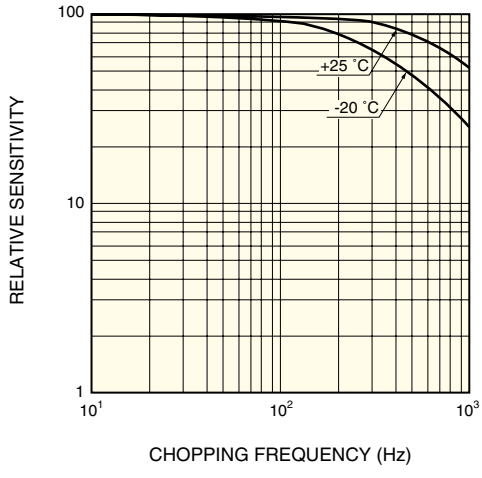

6-1-3 Linearity

Figures 6-5 and 6-6 show the relationship between the input energy and the output signal. The lower limit is determined by the NEP values of the PbS and PbSe respectively.

6-1-4 Temperature characteristic

Photo sensitivity, dark resistance and rise time of the PbS and PbSe vary with the temperature of the element, as shown in Figures 6-8 through 6-11.

Figure 6-8 Photo sensitivity vs. element temperature (PbS)

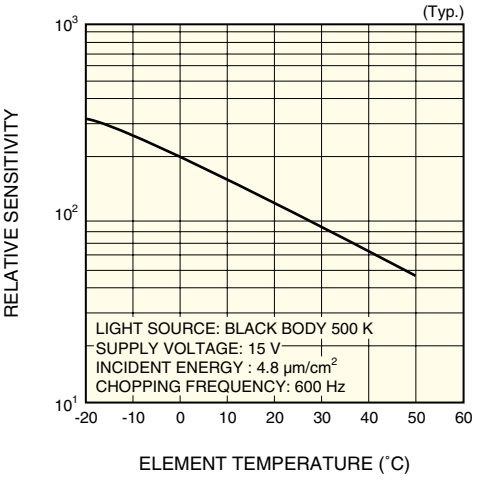

Figure 6-9 Photo sensitivity vs. element temperature (PbSe)

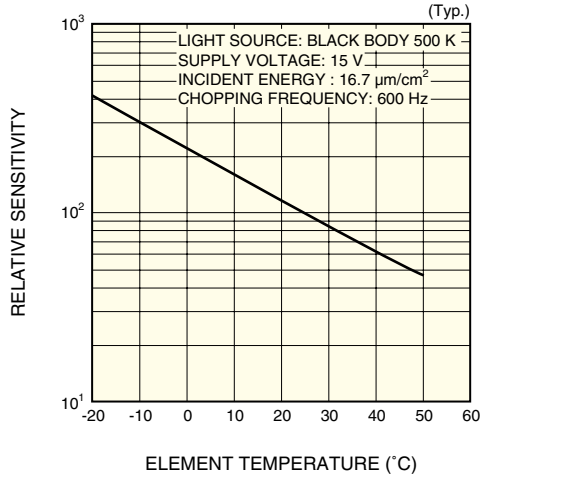

Figure 6-10 Dark resistance, rise time vs. element temperature (PbS)

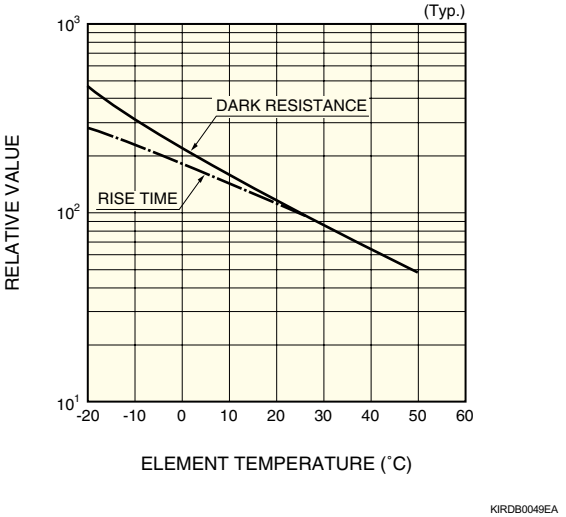

Figure 6-11 Dark resistance, rise time vs. element temperature (PbSe)

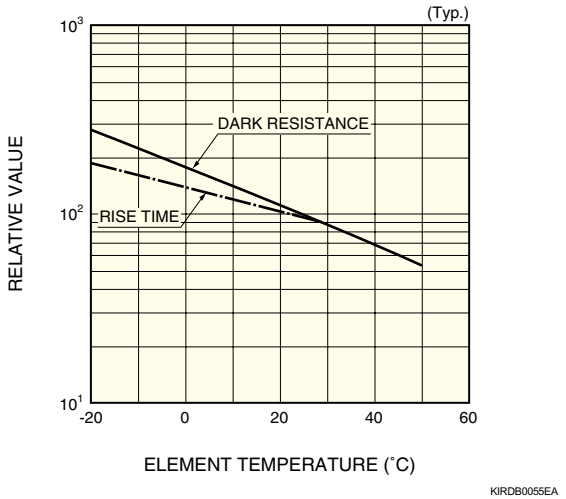

6-2 Precautions for circuit design

When operating a PbS or PbSe photoconductive detector, a chopper is used with the operating circuit to obtain AC signals, as shown in Figure 6-12.

Figure 6-12 Example of operating circuit

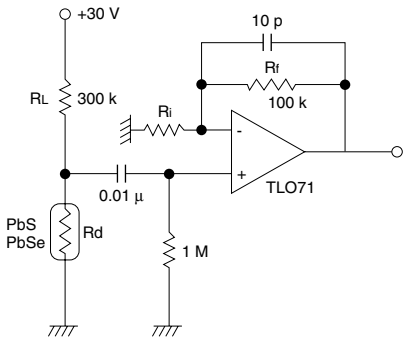

When the signal current as “is”, the signal voltage becomes as follows:

$$Vo = -is \cdot Rd\left(1 + \frac{Rf}{Ri}\right)$$

6-2-1 Temperature compensation

As stated in 6-1-4, “Temperature characteristics”, the photo sensitivity and dark resistance of PbS and PbSe change as the element temperature varies, so it is necessary to perform temperature compensation. One method is to use a thermistor appropriate to the PbS or PbSe being used. Hamamatsu thermoelectrically-cooled PbS detectors (P2532-01, P2682-01) and thermoelectrically-cooled PbSe detectors (P2038-03, P2680-03) incorporate a thermistor to keep the element temperature at a constant level. See Section 11, “Cooling techniques”, for information on how to use these cooled detectors. In some cases, the PbS and PbSe are used with a detecting element warmed by a heater and kept at a constant temperature, but this may reduce the photo sensitivity and accelerate deterioration of the detector element. Therefore, care should be taken when using this method.

6-2-2 Load resistance

When load resistance RL and dark resistance Rd are equivalent, the maximum signal can be obtained. The relation between the RL/Rd and the signal level is shown in Figure 6-13.

Figure 6-13 Output signal level vs. RL/Rd

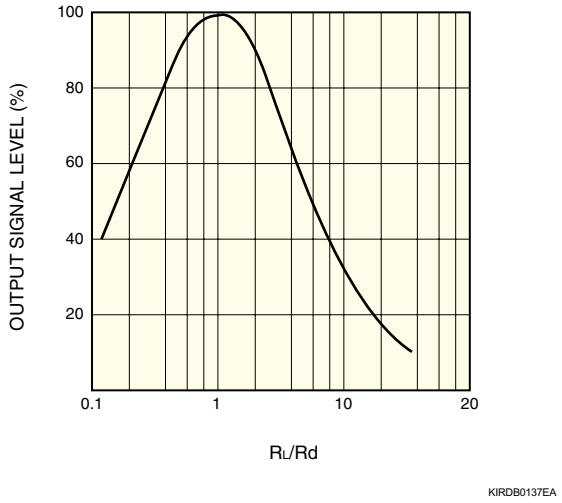

6-2-3 Chopping frequency

As stated in 6-1-2, “Time response characteristics”, D* is maximized when $f = \frac{1}{2\pi\tau}$.

Also, narrowing the bandwidth of the amplifier reduces the noise level and improves the S/N. For low-light-level measurements, the chopping frequency and the bandwidth must be taken into account.

6-2-4 Bias voltage dependence

The noise levels in the PbS and PbSe suddenly increase when the voltage applied to the detector elements exceeds a certain threshold level. Also, since the signal level increases in proportion to the voltage, it is recommended that the detectors be used at as low a voltage as possible within the rated maximum applied voltage described in the catalog.

6-2-5 Active area

With respect to the S/N, it is much more efficient to use PbS and PbSe with a small active area and introduce a converged light to the detector elements, rather than using detector elements with a large active area. Incident light may falls on the outside of the active area or extraneous light may enter the active area causing the S/N to drop. Take precautions against the optical path of the incident light.

7. InAs, InSb photovoltaic detector

Like InGaAs PIN photodiodes, InAs and InSb detectors are photovoltaic detectors having p-n junctions. Their spectral response ranges correspond to those of the PbS and PbSe detectors. Since the InAs and InSb detectors have faster response speeds and better S/N, they are used in different applications from the PbS and PbSe detectors.

7-1 Characteristics

7-1-1 Spectral response

InAs detectors are sometimes used at room temperatures for applications such as for laser detection and other special applications, but they are cooled with thermoelectric coolers, dry ice (-77 °C) or liquid nitrogen (-196 °C). Figure 7-1 shows the spectral response characteristics of the InAs detector and the InSb detector at a temperature of -196 °C.

Figure 7-1 Spectral response characteristics

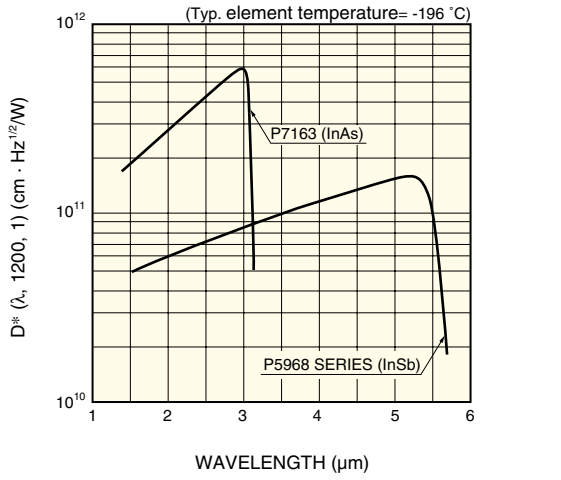

7-1-2 Noise characteristics

The InAs and InSb detectors are normally used at zero bias and only Johnson noise (ij) is considered as a major source of noise, which is expressed in terms of the following formula.

$$ij = \sqrt{4kTB / Rsh}$$

Also, in the spectral response range for the InSb detector, noise due to fluctuations in background light at a temperature of 300 K cannot be disregarded. If background radiant noise is thought to be the only noise source, D* for the photovoltaic detectors can be calculated using the following formula.

$$D^* = \frac{\lambda\sqrt{\eta}}{hc\sqrt{2Q}} \qquad [cm \cdot Hz^{1/2}/W]$$

- λ : wavelength
- η : quantum efficiency
- h : Planck constant
- c : light speed
- Q : background radiation flux [No. of photons/cm^2 · s]

To reduce the background radiant noise, it is necessary to employ a cold shield that restrains the field of view (FOV) and a cooled band-pass filter that cuts off wavelengths other than the wavelength of interest. The relation between FOV and D* is shown in Figure 7-3.

Figure 7-2 FOV

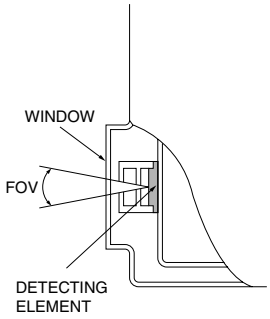

Figure 7-3 Relation between FOV and D*

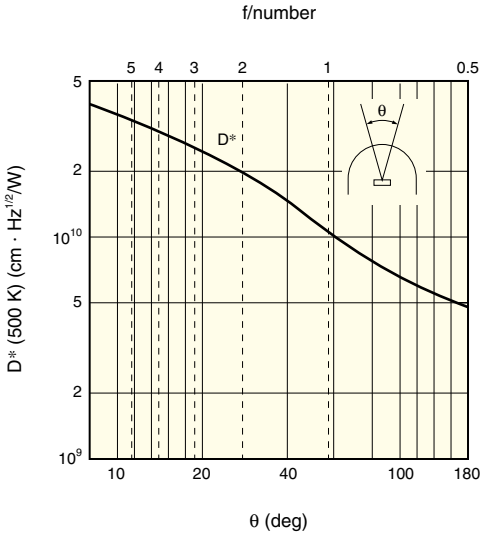

7-2 Precautions for use

Some precautions when using InAs and InSb detectors are described below. Also see Section 11-1, “Cooling by cryogen”, for cooling techniques using cryogen.

7-2-1 Dark current by visible light

When visible light or ultraviolet light other than infrared light to be measured enters the InSb detector, an electric charge accumulates on the surface of the detector element, increasing the amount of dark current. The increase in the dark current also increases the noise level of noise, and the S/N decreases. When using this type of light, put a cover (e.g. apply a double layer of black tape) on the incident window to keep out visible light (room illumination) and ultraviolet light. Then pour liquid nitrogen in the dewar container. If the dark current increases because the detecting element is exposed to visible light after pouring the liquid nitrogen, extract the liquid nitrogen to raise the element temperature back to room temperature. Then, when the above procedure is repeated, the dark current should return to the original value.

8. MCT, InSb photoconductive detector

Like PbS and PbSe photoconductive detectors, MCT (HgCdTe) and InSb photoconductive detectors are infrared detectors making use of the photoconductive effect that the resistance value of the detector element decreases when exposed to light.

8-1 Characteristics

8-1-1 Spectral response

The band gap of HgCdTe crystals depends on the composition ratio of HgTe to CdTe. This means that changing the composition ratio allows for production of infrared detectors having the maximum sensitivity at various wavelengths. Band gap Eg and long wavelength cut-off λc have the following relation.

$$\lambda c = \frac{1.24}{Eg\ (eV)} \qquad [\mu m]$$

In addition to the composition ratio, the band gap Eg changes with the detector element temperature. This relation is given by the following formula.

$$Eg = 1.59x - 0.25 + 5.23 \times 10^{-4}\, T(1 - 2.08x) + 0.327x^3$$

where x is the composition ratio as $Hg_{1-x}Cd_xTe$ and T is the absolute temperature. As the element temperature is raised, Eg increases and the peak wavelength shifts to the shorter wavelength region. Figure 8-2 shows the spectral response characteristics of MCT and InSb photoconductive detectors.

Figure 8-1 Energy gap vs. MCT crystal composition ratio [5)]

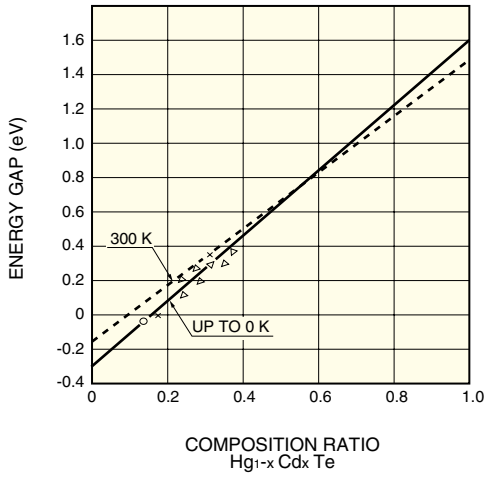

KIRDB0087EA

Figure 8-2 Spectral response

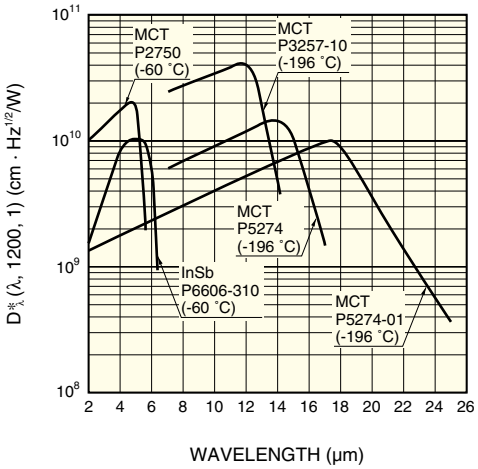

KIRDB0263EA

8-1-2 Noise characteristics

The noise of MCT and InSb detectors includes 1/f noise caused by current noise, g-r noise by recombination of electrons and holes, and Johnson noise as thermal noise. The 1/f noise is dominant in the low frequency region and the g-r noise is dominant in the higher frequency region. The relation between noise and frequency is shown in Figure 8-3. For MCT photoconductive detectors having sensitivity over 3 μm, fluctuations in background radiation at 300 K cannot be ignored as noise. This type of noise relates to FOV (field of view), and can be reduced by making the FOV smaller.

Figure 8-3 Noise vs. frequency

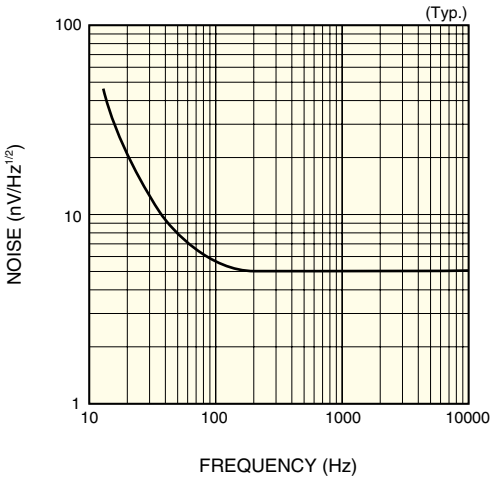

KIRDB0074EA

8-1-3 Temperature characteristics

The D* and spectral response characteristics of MCT photoconductive detectors change with the detector element temperature. As the temperature increases, the D* decreases and the spectral response shifts to the shorter wavelength region. Figures 8-4 and 8-5 show the D* of an MCT photoconductive detector designed for the 3 to 5 µm region and the temperature characteristic of the cut-off wavelength.
Figure 8-6 also shows the temperature characteristic of D* of an InSb photoconductive detector.

Figure 8-4 D* vs. element temperature (P2750)

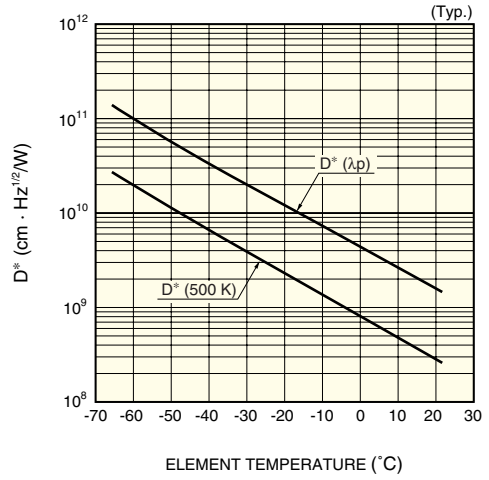

Figure 8-5 Peak sensitivity wavelength vs. element temperature (P2750)

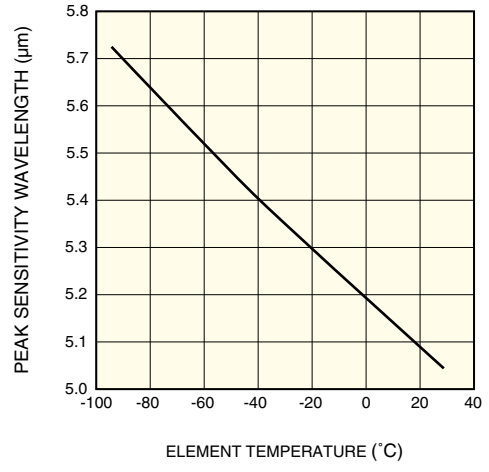

Figure 8-6 D* vs. temperature (P6606-310)

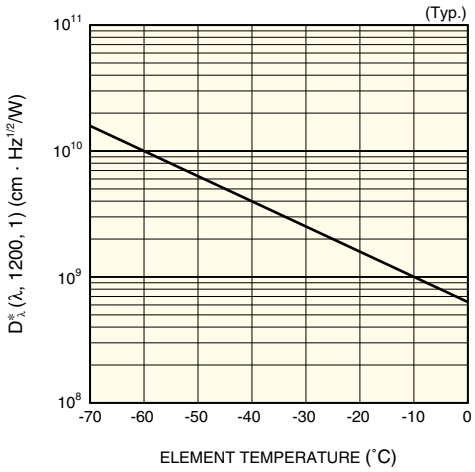

8-2 How to use the MCT detectors

8-2-1 Operation circuit

Figure 8-7 shows an example of the basic operation circuit for MCT photoconductive detectors. A power supply with low noise and ripple should be used. Normally, a resistance of several kilo-ohms is used as RL in many cases, to serve as a constant current source. As shown in Figure 8-8, as the bias current increases both the signal and noise increase, and at a certain level the S/N begins to drop sharply. The bias current must be set in the range where the S/N is constant. Setting the bias current higher than necessary may increase the detector element temperature due to Joule heat and results in a poorer D*. In worse cases, the detector element might be damaged.

Figure 8-7 Basic operation circuit

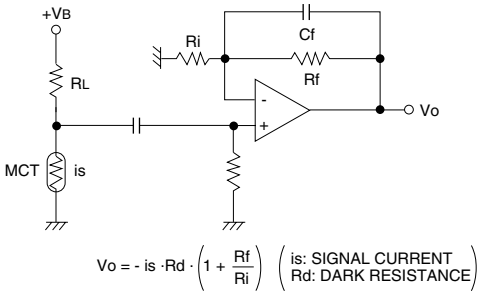

Figure 8-8 S/N vs. bias current (P3257-10)

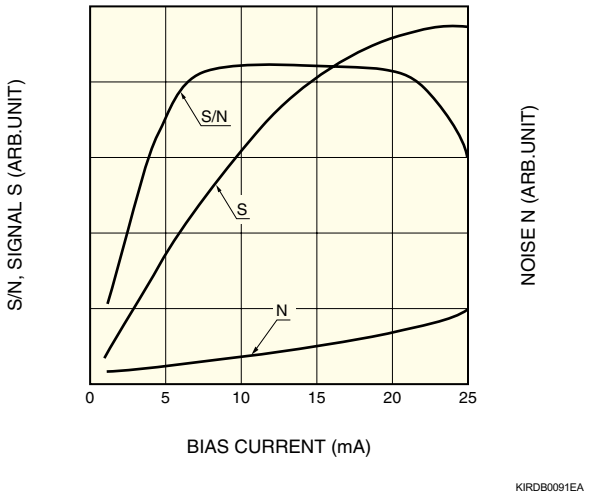

8-2-2 Ambient temperature

The sensitivity of MCT detectors may change as the ambient temperature changes. When the ambient temperature increases, the number of background photons increases, and accordingly the number of carriers inside the MCT detector element increases. This shortens the average life of the carriers excited by signal light and reduces the sensitivity. To prevent this phenomenon, optical systems must be designed carefully. For instance, the geometry of a cold shield should be designed so that the detector element is not exposed to unnecessary background radiation.

9. Pyroelectric detector

The pyroelectric detector is a thermal type infrared detector that operates at room temperatures. The pyroelectric detector consists of a PZT having the pyroelectric effect, a high resistor and a low-noise FET, hermetically sealed in a metal package to protect against external noise.
The pyroelectric detector itself does not have a wavelength dependence, but the combination of various window materials makes it usable for various applications, such as human body detection and gas analysis.

9-1 Pyroelectric effect

The PZT is spontaneously polarized in the dark state. The element surface is always electrified, but it is neutralized by ions in the air. When light enters the element and is absorbed, the element temperature increases, resulting in a change in the spontaneous polarization state. These changes are outputted as a voltage change. Since the pyroelectric detector detects light only when a temperature change in the element occurs, it is necessary to use an optical chopper for measurement of still objects. Figure 9-1 shows a schematic presentation of the pyroelectric effect.

Figure 9-1 Schematic presentation of pyroelectric effect

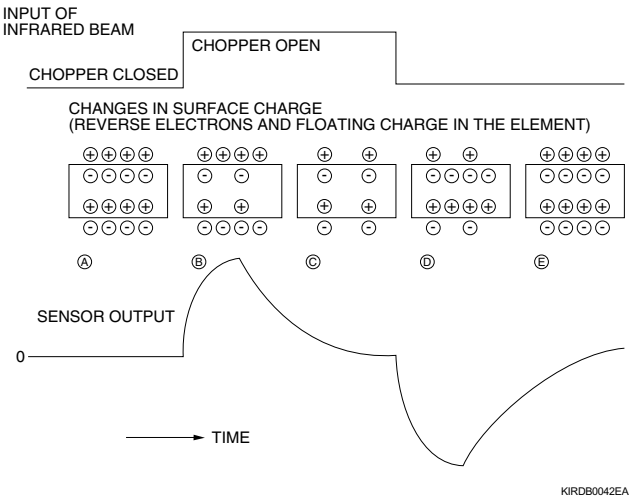

9-2 Pyroelectric materials

By changing the compositional ratio of PZT, various pyroelectric materials can be produced with a dielectric constant of 200 to 400 and a Curie temperature of 250 to 450 °C. Since PZT has a polycrystalline composition structure, it features high resistance to mechanical distortion caused by sudden temperature changes and offers extremely high stability against temperature fluctuations, allowing highly reliable operation as pyroelectric detectors. Table 9-2 shows typical characteristics of various pyroelectric materials.

Table 9-2 Characteristics of pyroelectric materials (p/C', $\varepsilon r^{1/2}$ and thermal conductivity K are included for reference)

Material name	Curie temperature TC (°C)	Dielectric constant ε_r	Pyroelectric coefficient p (10^{-8}C·cm^{-2}·K^{-1})	Volumetric specific heat C' (J·cm^{-3}·K^{-1})	Performance exponent P/C'·ε_r (10^{-10}C·cm·J^{-1})	P/C'$\varepsilon_r^{1/2}$ (10^{-10}C·cm·J^{-1})	Thermal conductivity K (10^{-3}·W·cm^{-1}·K^{-1})
TGS	49.5	38	3.5	2.4	4.3	24	6.4
DTGS	61	18	2.7	3.5	6.0	26	6.5 Max.
$LiTaO_3$	618	54	2.3	3.1	1.4	10	40
$Sr_{0.48}Ba_{0.52}Nb_2O_6$	115	380	6.5	2.3	0.73	14	
$PbTiO_3$ magnetic	460	190	1.8	3.2	0.30	4.1	32
$PbTiO_3$ light distribution film		97	3.0	≒3.2	0.97	9.5	
PZT (ceramic)	200 400	250 450	5.0 15	2.4	0.53	11	11.0
PVF_2	120	11	0.24	2.4	0.88	3.0	1.3

9-3 Operating principle

There are two methods for extracting a surface charge: using voltage, and using current. Ordinarily, voltage output type pyroelectric detectors are used. The voltage type offers a simple circuit configuration and less noise, and has a sensitivity peak at a relatively low frequency. Taking advantage of these features, it can be used in applications such as sensors to detect human bodies.
The current type features high gain and a constant sensitivity ranging from low to high, and is often used in laser detectors and other similar applications. The frequency limit is determined by the constant of the amplifier, so the frequency response can be improved by adjusting the circuit configuration of the amplifier.

9-3-1 Voltage type

The source follower circuit is generally used as a trans-impedance circuit. In this case, the voltage response Rv of the pyroelectric element is indicated by the equation shown below.

$$Rv = \frac{\eta\omega Ao\lambda}{G\sqrt{1+\omega^2\tau_t{}^2}} \times \frac{R}{\sqrt{1+\omega^2C^2R^2}}$$

$$= \frac{\eta\omega Ao\lambda R}{G\sqrt{(1+\omega^2\tau_t{}^2)(1+\omega^2\tau_e{}^2)}}$$

η : Emissivity
ω : Angular frequency
Ao: Active area
λ : Pyroelectric coefficient
R : Combined resistance (R ≒ Rg)
C : Composite capacity (C ≒ Cp+Cs)
G : Heat conductivity
H : Calorific capacity
τ_t : Thermal time constant (H/G)
τ_e : Electrical time constant (= C · R)
Rg: Resistor connected in parallel with pyroelectric element
Cp: Pyroelectric capacity
Cs : FET input capacity

Figure 9-3 Equivalent circuit using source follower circuit

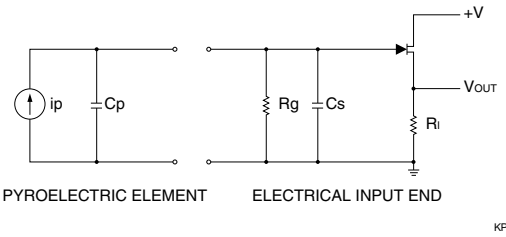

9-3-2 Current type

With this method, the surface charge on the pyroelectric element is output as current. The current responsivity Ri is expressed by the following equation.

$$Ri = \frac{\eta\omega Ao\lambda}{G\sqrt{1+\omega^2\tau_t{}^2}}$$

η : Emissivity
ω : Angular frequency
λ : Pyroelectric coefficient
Ao : Active area
R : Combined resistance (R + Rg)
G : Heat conductivity
H : Calorific capacity
τ_t : Thermal time constant (H/G)

In order to actually read the signal, a current/voltage converter circuit shown in Figure 9-4 is used.
When this circuit is used, the output voltage Vout is expressed as the sum of the current responsivity Ri and the feedback resistance Rf, using the equation given below.

$$VOUT = Ri \times Rf = \frac{\eta\omega Ao\lambda}{G\sqrt{1+\omega^2\tau_t{}^2}} \times Rf$$

Rf : Feedback resistance

Figure 9-4 Equivalent circuit for current/voltage converter using current-type pyroelectric element (typical example)

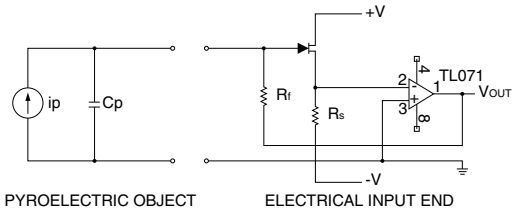

9-4 Characteristics

9-4-1 Frequency characteristics of voltage type

The sensitivity versus chopping frequency characteristics are shown in Figure 9-5 is expressed by its relationship with the electrical constant τe and the thermal time constant τt, and has the characteristic shown in Figure 9-5.

Figure 9-5 Voltage sensitivity vs. chopping frequency

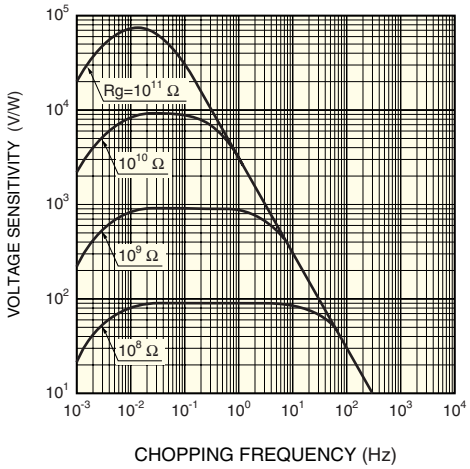

9-4-2 Frequency characteristic of current type

The sensitivity in relation to the chopping frequency is expressed by its relationship with the thermal time constant τt, and has the characteristic shown in Figure 9-6.

Figure 9-6 Current sensitivity vs. chopping frequency

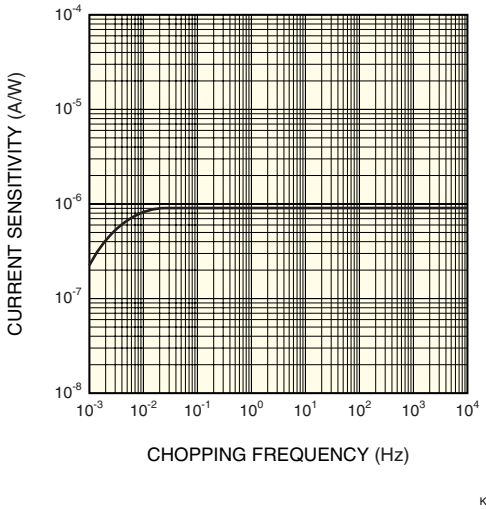

9-4-3 Field of view

The field of view (FOV) is defined as the angle where the sensitivity has fallen to 50 % of its maximum value. This is 100° for a single element and 120° for a dual element.

9-4-4 Spectral response

Since the pyroelectric detector is a thermal type detector, there is no wavelength dependency. The spectral response range is determined only by the window material used. Figure 9-7 shows typical spectral response characteristics of Hamamatsu pyroelectric detectors.

Figure 9-7 Spectral response characteristics

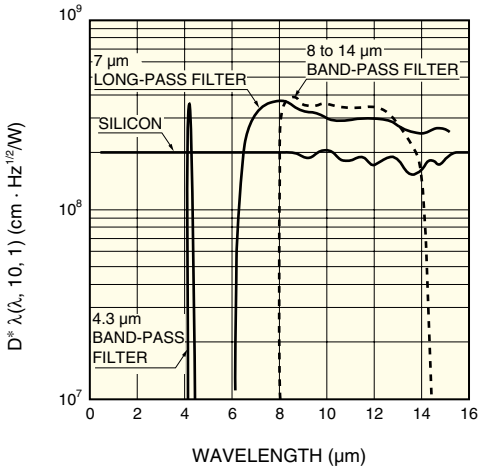

9-5 Features of voltage output type

Pyroelectric detectors (voltage output type) have the following features.

(1) Operation at room temperature

(2) Flat spectral response

(3) Output signal obtained only when there is a change in incident energy

(4) Built-in impedance-conversion FET

(5) Low cost

(6) Long life

(7) High sensitivity compared to other thermal type detectors

9-5-1 Single element and dual element

The equivalent circuits for the single element and dual element pyroelectric detectors are shown in Figure 9-8 (b). The dual element model is configured of two series-connected pyroelectric elements having opposite polarities, which utilize the cancellation effect of charges generated by background temperature variations such as by sunlight and external disturbance light and by vibration, thus preventing faulty operation. The single element type is generally combined with a chopper for use of radiation thermometers, etc. The dual type is mainly used for detection of moving objects such as human body sensing.

Figure 9-8 Equivalent circuits for pyroelectric detectors

(a) Single element

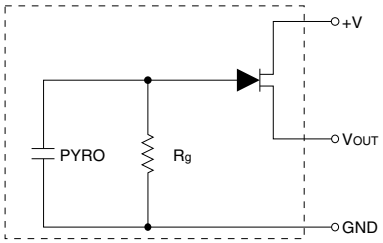

(a) SINGLE ELEMENT

(b) Dual element

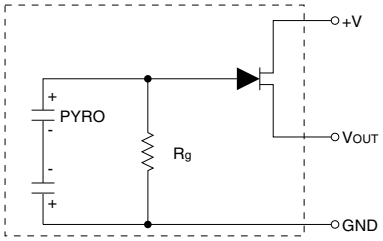

(b) DUAL ELEMENT

KPYRC0008EA

9-6 Operating circuits

Basic operating circuits are shown in Figure 9-9 (a) with preamplifiers using two power supplies and Figure 9-9 (b) with preamplifiers using a single power supply.
The optimum voltage to be applied to the pyroelectric element is 3 to 10 V.
Frequency responses of the amplifiers (a) and (b) are as expressed by formulas in the figures below.

Figure 9-9 Operating circuits of voltage output type

(a) Using two power supplies

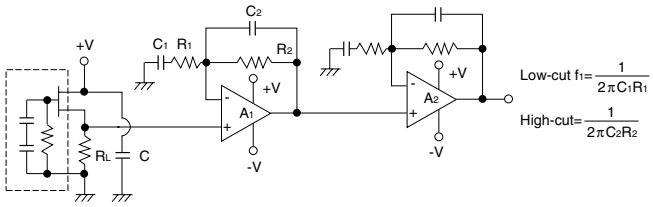

(b) Using a single power supply

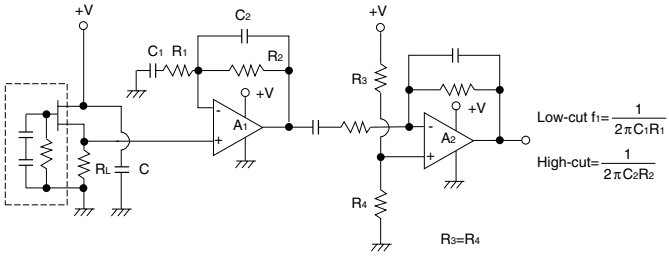

KIRDC0023EA

When operating using a single power supply, as shown in the circuit in (b), the operating position should be set to the center of the power supply voltage. In particular, if the first-stage amplifier is not AC-coupled, caution is required concerning this point. This operating position is determined by the voltage Voff generated at both ends of the load resistance RL when drain current flows.
Figure 9-10 shows an example of an operating circuit for a current-type pyroelectric detector. The low-frequency limit and high-frequency limit at that point can be determined in the same way as that shown in Figure 9-9 (a). In order to eliminate the effects of external noise, the pyroelectric element should be brought as close as possible to the first-stage amplifier.

Figure 9-10 Operating circuit example of current type

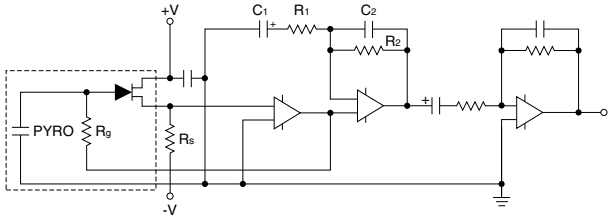

KPYRC0009EA

9-7 Environmental resistance

If the ambient temperature changes abruptly, the pyroelectric detector may malfunction. In particular, take sufficient precaution when pyroelectric detectors are used in locations exposed to air flow from an air conditioner. In this case, wrapping the detector with plastic or rubber as shown below will be effective.

Figure 9-11 Countermeasures against air flow

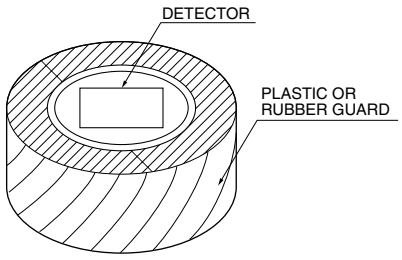

KPYRC0010EA

9-8 Fresnel lens

Pyroelectric detectors for human body detection are usually used in combination with Fresnel lenses. When designing Fresnel lenses, the following parameters should be taken into consideration.

Figure 9-12 Parameters for Fresnel lens design (unit: mm)

Parameter	Symbols in Figure 10-12
1. Detection distance	d_1, d_2
2. Field of view (1) Horizontal Center Upper & lower (2) Vertical Center Upper & lower	 θ_1, θ_2, θ_3, θ_4, etc 0° θ_5, θ_6, θ_7, θ_8, etc 0° θ_9, θ_{10}, etc
3. Lens dimensions	a × b
4. Lens material	—
5. Radius of curvature and length of lens	R, L
6. Material and thickness of window	—
7. Focal length	f
8. Installation height	h
9. Installation angle	θ
l0. Detector position inside lens	a_1, a_2, b_1, b_2

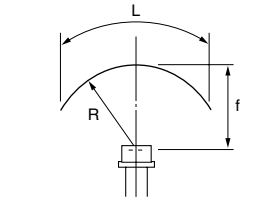

FOCAL LENGTH,
RADIUS OF CURVATURE, LENGTH

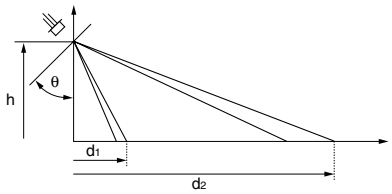

INSTALLATION AND DETECTION DISTANCE

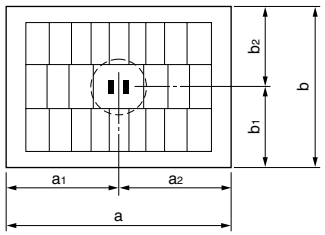

DETECTOR POSITION INSIDE LENS

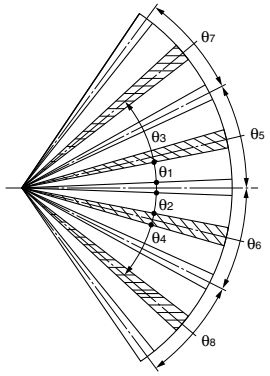

FIELD OF VIEW (HORIZONTAL FOV)

KPYRC0011EA

10. Two-color detector

To expand the spectral response range, two or more types of infrared detectors are sometimes stacked in a sandwich structure or arrayed on a plane. (These are often called two-color detectors). Examples of such arrangements of infrared detectors are shown in Figure 10-1. For two-color detectors, combinations of Si-PbS, Si-PbSe, Si-InGaAs, Si-Ge, Ge-InSb and InSb-HgCdTe are available from Hamamatsu. The upper detector also serves as a short-wavelength cutoff filter for the lower detector. These detectors can be more freely combined when arrayed on the same plane.

Figure 10-1 Example of two-color detector (unit: mm)

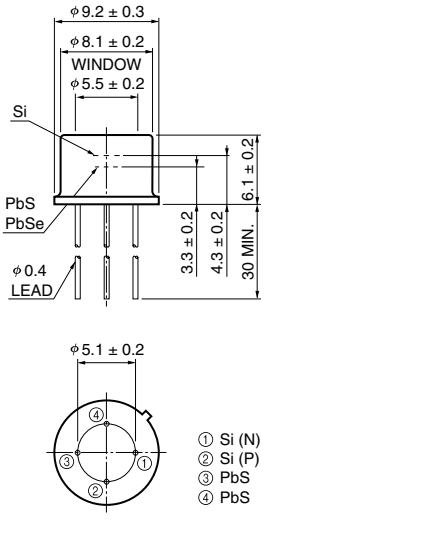

KIRDA0041EE

11. Cooling technique

Infrared detectors are cooled to improve the S/N or to keep the detector element at a constant temperature. There are various cooling techniques currently available, such as cryogenic dewar cooling using liquid nitrogen (-196 °C) or dry ice (-77 °C), thermoelectric cooling, Joule-Thomson cooling, and gas-circulation cooling.

11-1 Cooling by cryogen

For this cooling, a dewar infrared detector in which the detector element is fixed inside a glass or metal vacuum container is usually used. As cryogen, liquid nitrogen 77K (-196 °C) or dry ice 196K (-77 °C) is often employed. Generally, the detector can be operated for about 8 hours per filling of cryogen. The detector element temperature can be further decreased by de-compressing the cryogen inside the dewar.

Figure 11-1 Dimensional outline of glass dewar housing (unit: mm)

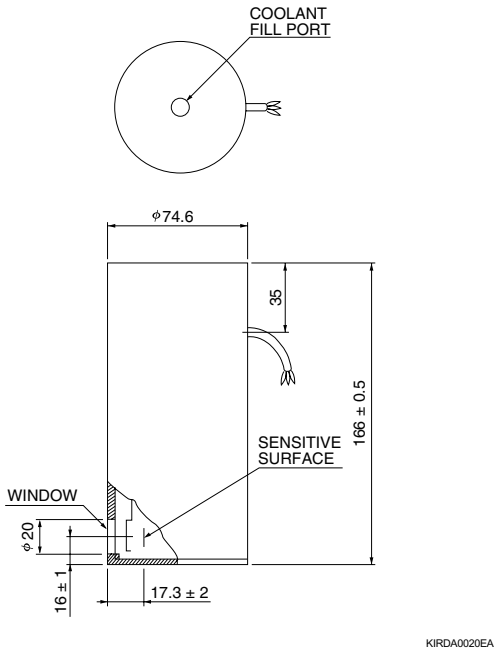

Figure 11-2 Pressure of cryogen vs. temperature [6)]

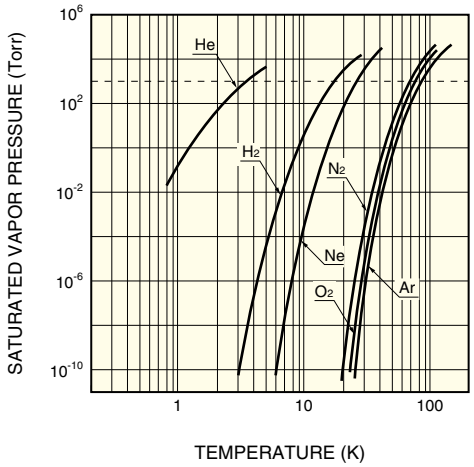

Some precautions for using dewar type infrared detectors are noted below.

(1) Do not apply excessive force to a glass dewar. When fixing the glass dewar detector, use the metal portion for fixing. A metal housing (A3262 series) designed for the glass dewar detector is also available from Hamamatsu.

(2) Wipe off water or moisture inside the dewar completely and then pour liquid nitrogen into it. Any remaining water or moisture could crack the dewar container.

(3) When using dry ice, crush it into grains and put them in a flask. Then pour alcohol onto the dry ice gently and mix them. After the dry ice becomes sherbet and stops boiling, gently fill the dewar container with the mixture, using a spoon.

(4) When handling liquid nitrogen, gently pour 20 to 30 cc into the dewar, and wait for a while until white vapor (caused by boiling of the liquid nitrogen) disappears. Then, pour another 20 to 30 cc, wait for a while again, and then pour as necessary. Pouring too much nitrogen from the beginning could cause a blowout. Also, if the liquid adheres to the outside surface of the dewar, the input window may become cloudy.

(5) For storage, keep the storage at as low a temperature as possible. If the storage temperature is too high, gas may be released from the inner wall of the dewar, reducing the degree of vacuum, so that the retention time of the cryogen is shortened. The vacuum life usually lasts approximately 3 to 5 years for a glass dewar and approximately 1 to 2 years for a metal dewar. The metal dewar container can be re-evacuated.

11-2 Thermoelectric cooler

When an electric current flows to a certain type of semiconductor, one end of the semiconductor is cooled and the other end is heated. This phenomenon is called "Peltier Effect". This Peltier effect can be used to cool the detector elements. (Figure 11-3)

Figure 11-3 Peltier effect

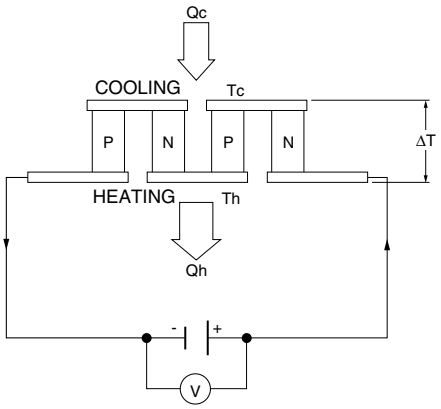

KIRDC0034EA

Thermometrically-cooled detectors use a one-stage, two-stage or three-stage thermoelectric cooler. Their respective temperature differences ΔTp between the cooling element and its package base are 50 °C, 70 °C and 100 °C. When air cooling is used, even though sufficient heat radiation is carried out, the base temperature becomes approximately 15 °C higher than the room temperature because of the thermal resistance between the base and the heatsink. Therefore the lowest element temperature that can be obtained at a room temperature of 25 °C is -10 °C for one-stage thermoelectric cooling, -30 °C for two-stage cooling and -60 °C for three-stage cooling. That is, their respective substantial temperature differences ΔT with regard to the ambient temperature are approximately 35 °C for one-stage thermoelectric cooling, 55 °C for two-stage cooling and 85 °C for three-stage cooling. Some precautions for use of the thermoelectrically-cooled detectors are summarized as follows:

(1) Always use a heatsink of less than 3 °C/W for one-stage and two-stage thermoelectric coolers, and less than 2 °C/W for three-stage thermoelectric coolers. Attach the heatsink tight fitting to the package base so that the base is efficiently heat-radiated. The cooling effect varies with the capacity of heatsinks used. Figure 11-4 shows one example of the cooling capability difference depending on the capacity of the heatsinks being used.

(2) Pay careful attention so that + and - are not reversed when connecting. If they are reversely connected and also if the temperature is suddenly increased, the infrared detector could be damaged.

(3) Use a power supply with low ripple.

(4) If a current higher than the specified value (1.5 A for one-stage thermoelectric coolers, 1.0 A for two-stage and three-stage thermoelectric coolers) flows, the infrared detector is heated by Joule heat. To use the detector in a stable condition for a long time, use it at 70 % of the specified value.

(5) Use a thermistor for temperature measurement within its rated value.

(6) When using a temperature controller, take into consideration the cooling capability of the cooling element, and set a control temperature that meets the conditions of the ambient temperature. Setting a temperature higher than the cooling capability ΔT will prevent stable temperature control. Hamamatsu provides the A3179 series heatsinks and the C1103 series temperature controllers.

Figure 11-4 Cooling capability of different heatsinks

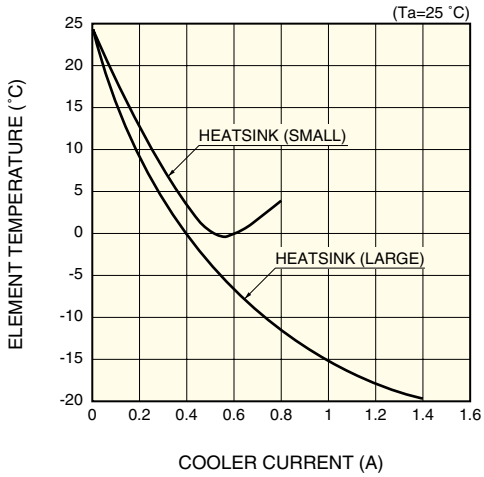

KIRDB0144EA

Figure 11-5 Cooling capability vs. power supply ripple

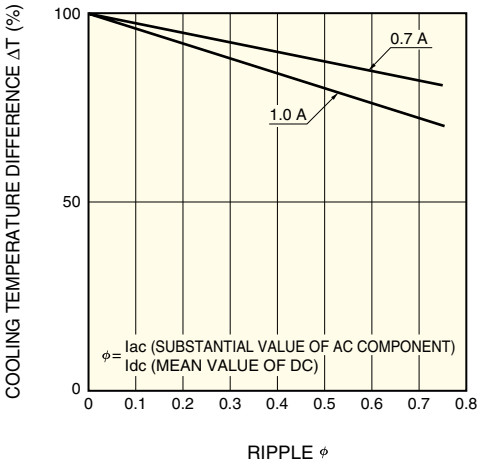

KIRDB0145EA

Figure 11-6 Block diagram for thermoelectric cooling

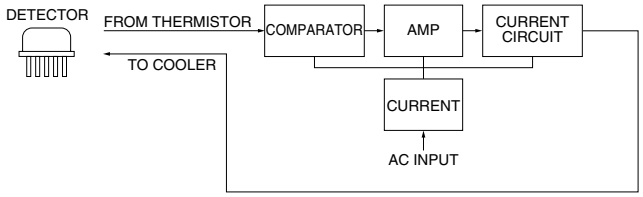

11-3 Joule-Thomson cooling

A temperature reduction takes place if a high pressure gas (e.g. 150 kg/cm^2, argon gas or nitrogen gas), is suddenly expanded, which is called the "Joule-Thomson effect". This Joule-Thomson effect can be used to cool detector elements to as low as the temperature of the cryogen.

Figure 11-7 Construction for Joule-Thomson cooling

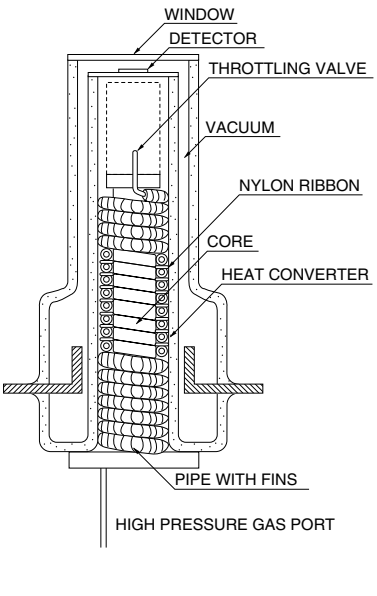

11-4 Gas-circulation cooling

As the Joule-Thomson cooling discharges the cooled gas, it is not suited for use over a long period of time. The gas circulation cooling, on the other hand, recollects the cooled gas and compresses it for reuse repeatedly, allowing for a long time use. The gas circulation cooling system consists of 3 units (expander, compressor and heat exchanger). The expander and compressor are divided into a rotary type using a turbine and a reciprocating type using a piston. The heat exchanger is divided into a thermal exchange type in which high and low pressure gases flow in different paths and a thermal storage type in which high and low pressure gases alternately flow in the same path. By combining these units, several gas-circulation systems are currently available, which are called Stirling, GM (Gifford McMahon), Solvey and Velmire. Among them, the Stirling cooler is the most suitable for cooling the infrared detector element as it is simple in structure and easy to reduce its size and weight. Disadvantages such as strong vibration and short service life have been greatly improved recently, so this cooling method is now widely used.

12. Applications of infrared radiation

12-1 Optical power meters

Optical power meters are used for measuring light intensity and find a wide variety of applications, such as in optical fiber communications and lasers. Optical fiber communications are classified into short, middle and long distance communications systems. For long distance optical communications systems, infrared beams in the wavelength region from 1.3 µm to 1.5 µm that provide less optical fiber transmission loss are employed. InGaAs PIN photodiodes, etc. are used for optical power meters to measure optical fiber transmission loss, relay quality, laser power, etc. The characteristics particularly required for the optical power meter are linearity and uniformity. Occasionally, a cooled-type detector is used to reduce the noise level so that low power light can be measured with low noise.

12-2 LD monitors

The output level and the emission wavelength of a laser diode (LD) vary with the temperature. To stabilize the LD, automatic power control (APC) is performed. The APC includes two methods: one is to monitor the integrated amount of light pulses from the LD and the other is to monitor the peak value of light pulses. With the development of high power LD, high linearity has become essential for monitoring light pulses. In the method for monitoring the peak value of light pulses, faster response is also required. InGaAs PIN photodiodes are mounted either in the same package as the LD or outside the package through an optical system. Also, both InAs and InSb detectors are used for longer wavelength lasers.

12-3 Radiation thermometers

Objects emit infrared radiation based on their own temperatures if they are above the absolute zero degree temperature. Figure 12-1 shows the radiant energy of a black body. Actually, the quantity of infrared rays emitted from an object is not necessarily determined based on the temperature. The emissivity e must be compensated for. In the case of a black body, e = 1. Figure 12-2 shows the emissivity of various objects. Since the emissivity e is determined by the temperature and wavelength of an object, care should be taken when measuring the absolute temperature of an object.
Generally, the noise equivalent temperature differential (NEΔT) is used as an index to express the thermal resolution. The NEΔT is defined as follows:

$$NE\Delta T = \frac{L_N}{\left.\frac{dL}{dT}\right|_{T = T_1}}$$

L_N: Noise equivalent luminescence
L : Radiance of object
T_1 : Temperature of object

The L_N has the following relationship with the NEP of the sensor:

$$NEP = To L_N \Omega Ao / \gamma$$

To : Optical system loss
Ω : Solid angle at which object is seen from the optics system
Ao: Aperture of optical system
γ : Circuit loss

Also, the equation $\left.\frac{dL}{dT}\right|_{T = T_1}$ expresses the temperature coefficient of the radiance of an object at temperature T_1, and L is obtained by accumulating the spectral radiant emittance across the observation wavelength area (λ_1 to λ_2).

$$L = \int_{\lambda_1}^{\lambda_2} \frac{1}{\pi} M\lambda d\lambda$$

M_1: Spectral radiant emittance

Compared to other temperature measurement methods, radiation thermometers have the following features:

(1) Measurement without direct contact with the object

(2) Faster response

(3) Easy pattern measurements

The detectors used for radiation thermometers must be selected based on the temperature and material of the object to be measured. For example, the glass has a peak wavelength of emissivity ε near 5 µm and plastic films near 3.4 µm or 8 µm. Therefore, detectors sensitive to such wavelength regions must be selected for those objects. Also, as a result of recent developments in infrared fibers, infrared detectors combined with infrared fibers are used in diverse applications, including temperature measurement of hot metal detectors (HMD) and other objects which rotate, have a complex internal structure and are located in dangerous environments such as vacuums and high-pressure gases.

Figure 12-1 Blackbody spectral radiant emittance

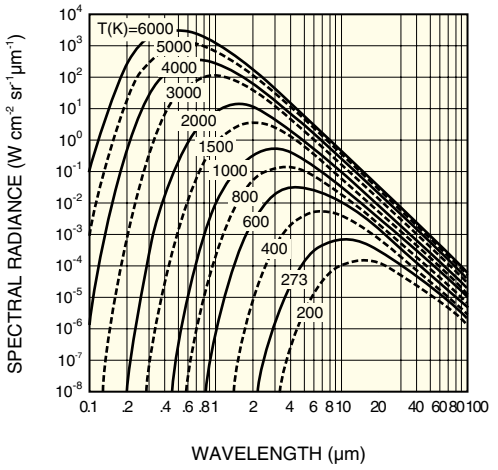

KIRDB0014EB

Figure 12-2 Emissivity of various objects [7)]

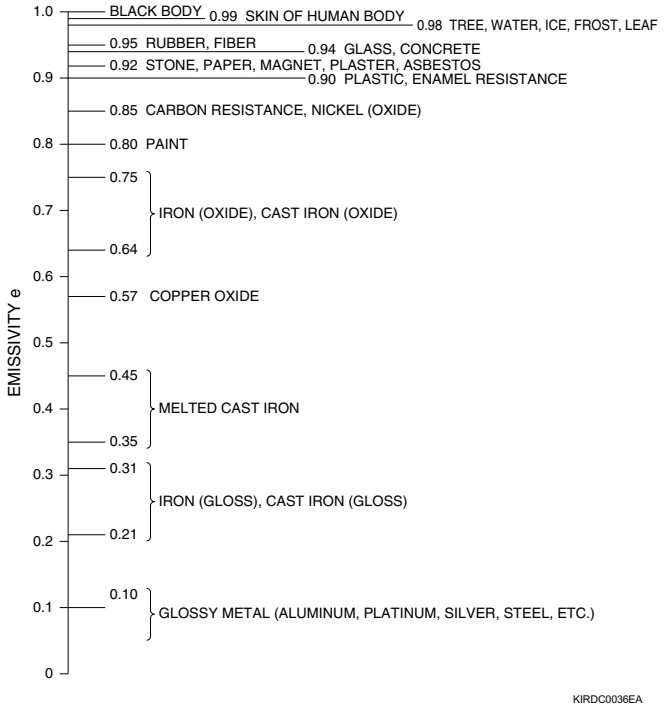

KIRDC0036EA

Figure 12-3 Transmittance and reflectance of glass

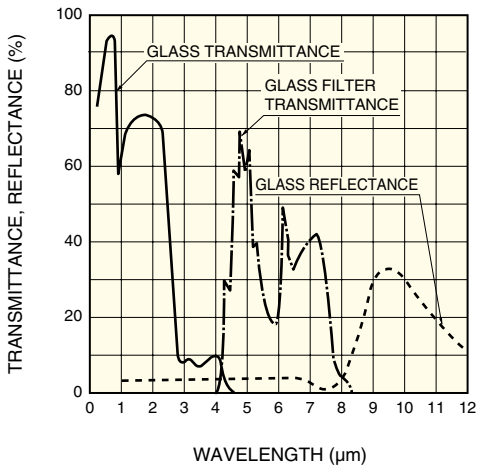

KIRDB0146EA

12-4 Flame monitors (flame detection)

The flame monitor is used for detecting light emitted from flames and for observing how the flames are burning. As shown in Figure 12-4, light emitted from flames is distributed widely from the UV region to the infrared region. Detection methods include using a PbS photoconductive detector to detect infrared light, using a two-color detector (K1713-01) to detect a broad spectrum from the UV region to the infrared region, and using PbSe and pyroelectric detectors to detect a wavelength of 4.3 μm.

Figure 12-4 Emission from flames

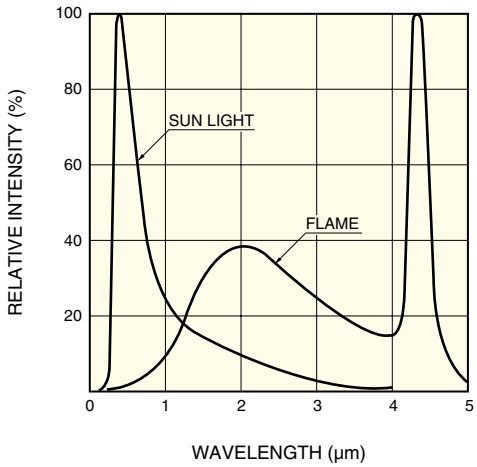

KIRDB0147EA

12-5 Moisture analyzers

The water content or moisture analyzer uses wavelengths (1.1 μm, 1.4 μm, 1.9 μm, 2.7 μm) that are absorbed by moisture in the infrared region. Light beams at these wavelengths and reference wavelength are irradiated on an object such as vegetable or coal, and the moisture analyzer receives the reflected or transmitted light from the object and calculates the ratio to the reference wavelength light to measure the moisture. InGaAs PIN photodiodes and PbS photoconductive detectors are suitable for sensors in this application.

12-6 Gas analyzers

Gas analyzers make use of absorption in the infrared region of gases and measure the gas density. There are two methods called the dispersive and the non-dispersive methods. The dispersive method spectroscopically divides infrared light emitted from a light source into spectra and uses their absorption characteristics to measure the ingredients and quantity of a sample. The non-dispersive method measures only the absorption characteristics, but is more commonly used than the dispersive method. For example, non-dispersive infrared gas analyzers are used for measurements of automobile exhaust gases (CO, HC, CO_2), intake gas (CO_2), emission controls (CO, SO, NO_2), fuel leakages (CH_4, C_3H_2), and so on. Ingredient analyzers are used to measure CO_2 (4.3 μm) and saccharine (3.9 μm) in carbonated drinks (soft drinks, beer, etc.). Figure 12-5 shows typical absorbed spectra of various gases.

Figure 12-5 Gas absorption spectra

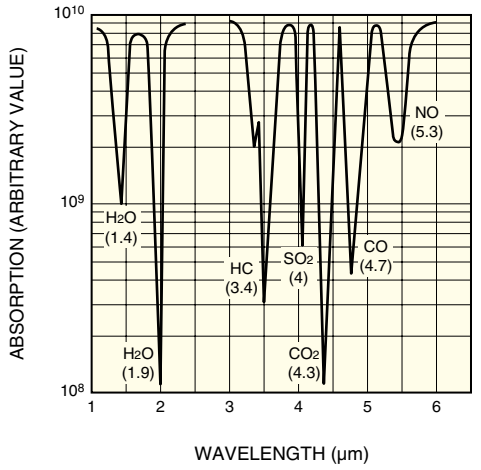

KIRDB0148EA

12-7 Infrared imaging devices

Development of infrared imaging devices are classified into 1st, 2nd and 3rd generations in the course of development, as shown in Figure 12-6. In the 1st generation, since only a single detector element is used, the optical system is required to rotate around the X axis and Z axis to create an image. A linear array (1D array) is used in the 2nd generation, so the optical system has only to rotate around the Z axis. In the 3rd generation, an area array (2D array) is used, so that there is no need to scan an infrared image using the optical system. Figure 12-7 shows an example for the infrared imaging device. If an element array is used for the infrared imaging device, its optical system can be simplified, so the device becomes compact and light-weight. However, the characteristic difference between each element might be a problem. The infrared imaging device is used in a wide variety of applications in the fields of industry, medicine and science, as shown in Table 12-1.

Figure 12-6 Schematic diagram of infrared imaging device [9)]

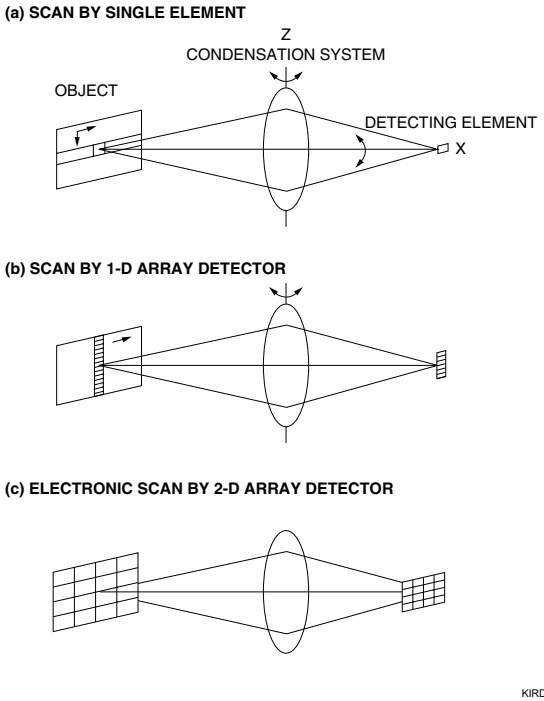

KIRDC0037EA

Figure 12-7 Configuration example of infrared imaging device

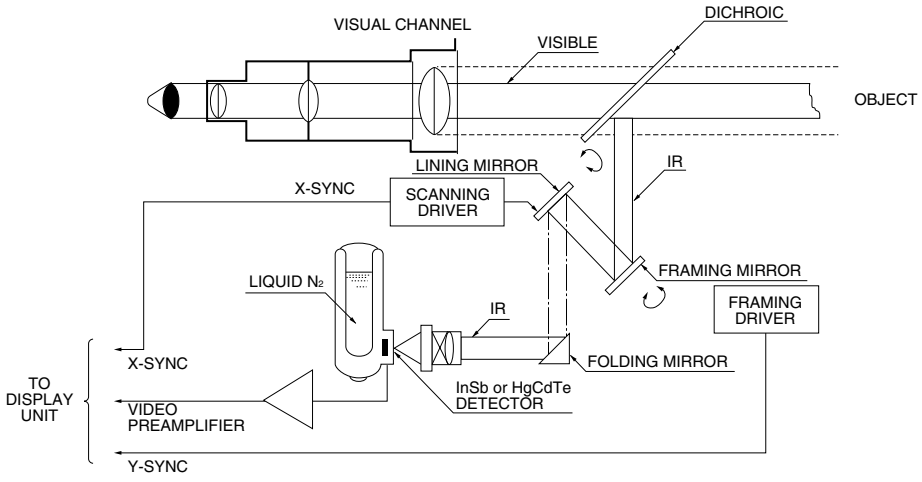

KIRDC0038EA

Table 12-1 Applicable fields of infrared imaging device [10)]

Industrial use	Heat treatments for steel, non-ferrous metal, rubber, paper, etc. Tests and control for the process of such materials. Destruction tests for blowholes of cast iron, welded and soldered parts. Tests for screening of printed circuit boards. Tests for engine performance of automobile, airplane, etc. Maintenance and inspection for generator, converter and junctions of power cable, etc. Monitors for heat and heat distribution by bearing, cutting, rolling, etc.
Other industrial use	Marine use such as fish detection Agricultural use such as detection of damaged areas by harmful insects
Environmental pollution use	Seawater pollution by oil, hot water, etc.
Scientific research use	Surveys for soil, water resources, water currents, volcanos, meteorological phenomena, etc.
Medical use	Infrared imaging diagnosis (e.g., medical thermograph)
Security use	Monitor for abnormal heat leakage from blast furnace, boiler, heat treatment furnace, etc. Fire detection, intruder detection, etc.

12-8 Remote sensing

Objects emit or reflect light as shown in Figure 12-9, and such light includes different information, depending on the wavelengths. By measuring each wavelength, specific information about the objects can be obtained. The infrared remote sensing allows us to obtain more specific information such as the surface temperatures of solids and liquid, types and temperatures of gases, etc. Particularly, with the growing use of remote sensing by space satellites and airplanes in the past years, we are now able to obtain macroscopic information such as the temperatures of land and seawater, the gas concentration in atmosphere, etc. Such information has been utilized for meteorological observation, environmental pollution monitoring, resource detection, etc.

Figure 12-9 Optical system for resource detection [8)]

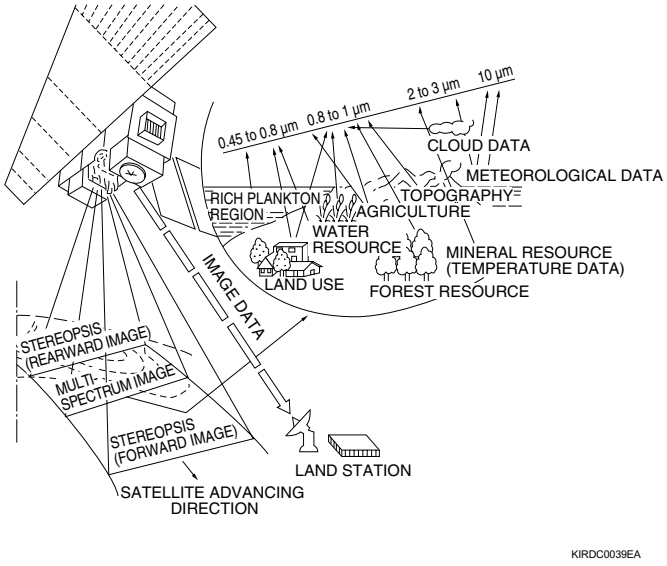

12-9 Sorting devices

By making use of the absorption wavelength inherent to organic matter, it is possible to sort agricultural crops (such as potatoes, tomatoes, onions and garlic) from clods and stones. InGaAs PIN photodiodes and PbS photoconductive detectors are used for such sorting. Also, those detectors are used to sort products on the belt conveyor of a factory by detecting the differences of temperature, emissivity, transmittance.

12-10 Human body detection

12-10-1 Intrusion alarm device

When the temperature of a moving human body is detected, this device outputs a warning signal. Infrared radiation emitted by the intruder is collected by the detector, using a mirror or a Fresnel lens. To cover a wide range must, a multiple-surface mirror or Fresnel lens array is used. If the speed at which the person moves is converted into frequency, it is about 0.3 Hz for tiptoeing and about 10 Hz for outright dash. (Figure 12-10)

The temperature emitted from the human body may change depending on clothing and the season, and ranges from 20 to 30 °C, as shown in Table 12-2. It corresponds to a blackbody radiation having a peak of 9.5 µm.

Optical filters that transmit wavelengths from 7 to 15 µm are used as the window material so as to make use of a window in the atmosphere, to select the wavelength region suitable for the human body temperature and to avoid effects from the external disturbance light such as sunlight.

Figure 12-10 Moving speed of person and frequency [10)]

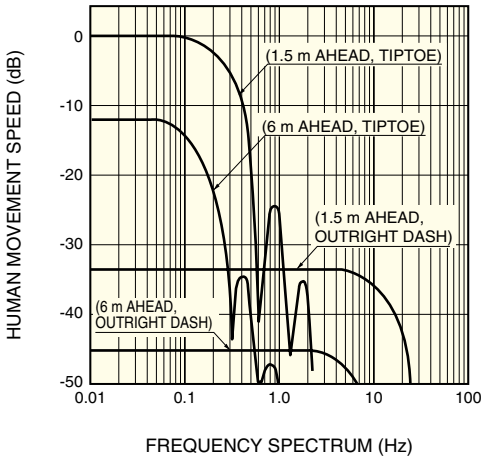

Table 12-2 Temperature of human body

	Winter clothes (4 outer layers, 3 under layers)	Summer clothes (2 outer layers, 2 under layers)
Face	31.2 ˚C	32.0 ˚C
Back of head	23.4 ˚C	30.9 ˚C
Chest	20.9 ˚C	29.3 ˚C
Back	20.9 ˚C	29.0 ˚C
Stomach	22.2 ˚C	30.5 ˚C
Hip	20.4 ˚C	31.0 ˚C
Thigh	21.3 ˚C	28.6 ˚C
Shin	21.3 ˚C	28.4 ˚C

Measured with a radiation thermometer.

12-10-2 Auto light switches

When a person enters a dark place, this device detects the person's entrance and turns on the light. The principle of this device is the same as that of the intrusion alarm device. Figure 12-11 shows one example of the circuit configuration.

13-10-3 Automatic doors

Pyroelectric infrared detectors are also used for the passive type of automatic door opener. In comparison with the active ultrasonic type, it is advantageous as its circuit configuration is simple, thus allowing a low cost for the system.

Figure 12-11 Circuit example for light switch [11)]

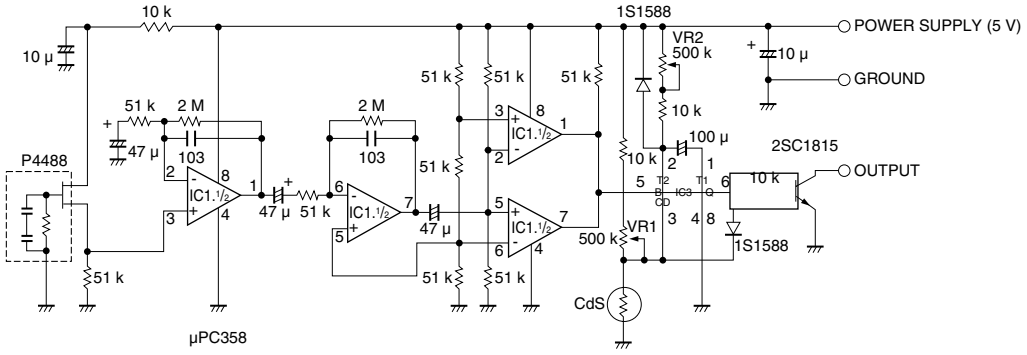

12-11 Spectrophotometers (FT-IR)

Dispersive spectrophotometers have conventionally been popular, but recently use of Fourier transform infrared (FT-IR) spectrophotometry has been increasing. In FTIR spectrophotometry, an interference signal obtained with a double beam interferometer undergoes Fourier transformation by which the signal is decomposed into a spectrum. This method has the following features.

1. **Multiple spectral elements are simultaneously measured with high S/N.**
2. **High wavelength accuracy because of wavelength determination laser light.**
3. **Useful in the infrared region where the luminance of a light source is low and highly sensitive detectors such as photomultipliers are not available.**

Infrared detectors used as the heart of the FT-IR spectrophotometers must have the following characteristics.

(1) Wide spectral response range

(2) High sensitivity

(3) Large active area enough to satisfy bright optical systems

(4) Wide frequency bandwidth

(5) Good linearity over wide incident light levels.

Thermal type detectors are mainly used over a wide wavelength region of from 2.5 to 25 μm. For measurements requiring high sensitivity and high-speed sampling or using small amounts of samples, MCT (HgCdTe) photoconductive detectors and InSb photovoltaic detectors are used.

References

1) Komoto; Material Science (Japanese) , 14 (1977), P267

2) H.A. Gebbie et al.; Proc. Roy. Soc., A206 (1951), AP87

3) Okuda, Shibai; Infrared Technology (Japanese) 11 (1986), P4

4) Yoshida; Optical Technology Contact (Japanese) 24 (1986), P681

5) D. Long; Energy Bands in Semiconductors (1968), Wiley, N.Y.

6) Otsuki; Infrared Technology (Japanese) 8 (1983), P73

7) Miyauchi; Sensor Techonology (Japanese), 15 (1985) Oct. P48

8) Kudo, Nakura; Infrared Technology (Japanese) 11 (1986), P73

9) R. F. Leftwich; SPIE 62 (1975), P217

10) Ishii; Infrared Technology Research Meeting Proceeding (Japanese) No.64 (1978)

11) Kurahashi; Optoronics (Japanese) 4 (1988), P123

HAMAMATSU PHOTONICS K.K., Solid State Division
1126-1 Ichino-cho, Higashi-ku, Hamamatsu City, 435-8558 Japan, Telephone: (81) 53-434-3311, Fax: (81) 53-434-5184, http://www.hamamatsu.com
U.S.A.: Hamamatsu Corporation: 360 Foothill Road, P.O.Box 6910, Bridgewater, N.J. 08807-0910, U.S.A., Telephone: (1) 908-231-0960, Fax: (1) 908-231-1218
Germany: Hamamatsu Photonics Deutschland GmbH: Arzbergerstr. 10, D-82211 Herrsching am Ammersee, Germany, Telephone: (49) 08152-3750, Fax: (49) 08152-2658
France: Hamamatsu Photonics France S.A.R.L.: 19, Rue du Saule Trapu, Parc du Moulin de Massy, 91882 Massy Cedex, France, Telephone: 33-(1) 69 53 71 00, Fax: 33-(1) 69 53 71 10
United Kingdom: Hamamatsu Photonics UK Limited: 2 Howard Court, 10 Tewin Road, Welwyn Garden City, Hertfordshire AL7 1BW, United Kingdom, Telephone: (44) 1707-294888, Fax: (44) 1707-325777
North Europe: Hamamatsu Photonics Norden AB: Smidesvägen 12, SE-171 41 Solna, Sweden, Telephone: (46) 8-509-031-00, Fax: (46) 8-509-031-01
Italy: Hamamatsu Photonics Italia S.R.L.: Strada della Moia, 1/E, 20020 Arese, (Milano), Italy, Telephone: (39) 02-935-81-733, Fax: (39) 02-935-81-741

Cat. No. KIRD9001E03
Nov. 2004 DN